Characterisation of air masses passing over the Vredefort Dome world heritage site

M Dunn

22120017

Dissertation submitted in fulfilment of the requirements for the degree *Magister Scientiae* in Environmental Sciences (Specialising in Chemistry) at the Potchefstroom Campus of the North-West University

Supervisor: Prof JP Beukes

Co-supervisor: Dr PG van Zyl

November 2015

Acknowledgements

I would firstly and most importantly like to thank my Father in Heaven for granting me the opportunity, the strength and the knowledge to complete my MSc.

Isaiah 40:31. "but those who hope in the LORD will renew their strength. They will soar on wings like eagles; they will run and not grow weary, they will walk and not be faint."

I would also like to thank:

My husband, Andrew, for his willingness to help me with my MSc, his encouragement and his loving support.

My mother and my brother, Ilze and Henri, for making me what I am today and their love, encouragement and support.

My supervisors, Prof Paul Beukes and Dr Pieter van Zyl, for their support, guidance, encouragement and assistance.

My friends and family for their prayers, support and love.

Preface

Introduction

This dissertation was submitted in article format, as allowed by the North-West University (NWU). This entails that the article is added into the dissertation as it was submitted for review to the journal. The conventional "Results and discussions chapter" was therefore replaced by the article. Separate background and motivation (Chapter 1), literature (Chapter 2), experimental (Chapter 3) and project evaluation (Chapter 5) chapters were included in the dissertation, although some of this information was summarised in the article. This will result in some repetition of ideas/similar text in some of the chapters and in the article. The numbering of Chapter 4 (that contains the article) is also not consistent with the rest of the dissertation, since it was added in the exact format as it was submitted to the journal. The figures and tables of Chapter 4 are also added at the end of the text, as prescribed by the journal.

Rationale in submitting dissertation in article format

It is currently a prerequisite at the NWU for submission of an MSc dissertation that a draft article must be prepared. Many of these draft papers are never submitted to national and international accredited peer reviewed journals. However, the candidate decided to submit this MSc dissertation in article format, since it required that the candidate prepare a paper that was submitted to an ISI-accredited journal. Therefore, the prerequisite of the NWU was exceeded.

The co-authors of the above-mentioned article (Chapter 4) were:

Marcell Venter[1], Johan Paul Beukes*[1], Pieter Gideon van Zyl[1], Andrew Derick Venter[1], Kerneels Jaars[1], Miroslav Josipovic[1], Markku Kulmala[2], Ville Vakkari[3], Lauri Laakso[1,3]

1 Unit for Environmental Sciences and Management, North-West University, Potchefstroom, South Africa

2 Department of Physics, P.O. Box 64, FIN-00014, University of Helsinki, Finland

3 Finnish Meteorological Institute, Helsinki, Finland

Contributions to article

Contributions of the various co-authors were as follows. The bulk of the work was done by the candidate, Marcell Venter, with conceptual ideas and recommendations by the study leaders JP Beukes and PG van Zyl. AD Venter, K Jaars and M Josipovic assisted in data collection at the Welgegund measurement station, while M Kulmala, V Vakkari and L Laakso assisted in creating the infrastructure at Welgegund, as well as making conceptual contributions.

Formatting and current status of article

The article was formatted in accordance with the journal specifications, i.e. *South African Journal of Science*. The author's guide that was followed in preparation of the article was available at http://www.sajs.co.za/guidelines-authors (Date of access: 12 April 2016).

Consent by co-authors

All the co-authors on the article (Chapter 4) have been informed that the MSc dissertation will be submitted in article format and have given their consent.

Abstract

In 2007, it was announced that the Vredefort Dome will be proclaimed South Africa's seventh UNESCO (United Nations Educational, Scientific and Cultural Organisation) world heritage site. It is the largest and second oldest meteorite impact structure in the world and is situated in the Witwatersrand basin (containing ~40% of the world's gold resources). In addition to the economic importance of the Vredefort Dome, it is of great geological (e.g. large meteorite crater with inverted sedimentary structures); cultural and historical (e.g. stone age caves with tools and human remains, Khoi-San rock art, remnants of the Anglo-Boer war and old gold mines); conservational (e.g. diverse indigenous plant, animal and bird species, as well as water quality associated with the Vaal river); and aesthetic (e.g. providing unique scenery with associated ecotourism opportunities) significance in South Africa.

Air quality in the Vredefort Dome can potentially be affected by the nearby declared air pollution priority areas, i.e. the Vaal Triangle Airshed Priority Area (VTAPA), the Highveld Priority Area (HPA) and the Waterberg Priority Area (WPA), as well as the Johannesburg-Pretoria (Jhb-Pta) megacity, which is well-known for high levels of atmospheric pollution. Notwithstanding the national and international importance of the Vredefort Dome, as well as the proximity of the afore-mentioned polluted source regions, currently, no air quality data is available for this area. The management plan, as required by the UNESCO declaration, also highlighted this deficiency.

In an effort to partially address the air quality knowledge gap, air masses from 1 June 2010 to 28 February 2014 passing over the Vredefort Dome were isolated and analysed at the Welgegund atmospheric measurement station as a proxy for ground-level air quality over the Vredefort Dome. Atmospheric species reported on in this thesis are in accordance with the National Ambient Air Quality Standards (NAAQS). The proxy method applied had some

limitations, since the frequency of such back trajectories was limited and those that did comply passed mostly over the cleaner south-western sector from the Vredefort Dome. Additionally, dilution during transport and aging of air masses after passing over the Vredefort Dome before arriving at Welgegund could also affect the pollutant levels observed.

By comparing the results with South African air quality standards, it is evident that O_3 and PM_{10} exceeded the South African air quality standard limits. O_3 is a regional problem, while PM_{10} mostly originates from industries, household combustion and savannah/grassland fires. Although there were no exceedances recorded for SO_2 and NO_2 in air masses complying with the selection criteria, it is highly likely that such exceedances will occur over the Vredefort Dome. It is suggested that emission interventions for industrial activities, the vehicular fleet, as well as savannah and grassland fires be done in order to address species of regional concern. In order to address household combustion emissions, social and economic transformations in South Africa need to be accomplished, which are linked to the economic success and -growth of the country.

Keywords: Vredefort Dome, World heritage site, Air quality, Welgegund, South Africa

Index

List of abbreviations

BC:	Black Carbon
CCN	Cloud Condensation Nuclei
EPA	Environmental Protection Agency
HPA	Highveld Priority Area
IN	Ice Nuclei
IPPC	Intergovernmental Panel on Climate Change
MAAP	Multi-Angle Absorption Photometer
NAAQS	National Ambient Air Quality Standards
OC	Organic Carbon
PGM	Platinum Group Metals
PM	Particulate Matter
PMT	Photomultiplier Tube
SHARP	Synchronized Hybrid Ambient Real-time Particulate Monitor
UNESCO	United Nations Educational Scientific and Cultural Organisation
VTAPA	Vaal Triangle Airshed Priority Area
WHO	World Health Organisation
WPA	Waterberg Priority Area

List of figures

Chapter 2

Chapter 3

List of tables

Chapter 2

Chapter 1

Background, motivation and objectives

1.1. Background and motivation

In 2007, it was announced that the Vredefort Dome will become South Africa's seventh UNESCO world heritage site (UNESCO, 2015; SA, 2007). The Vredefort Dome is located on the boundary between the North West and the Free State Provinces. It is known as the largest (diameter of 160 km) and the second oldest (~2023 Ma) meteorite impact structure in the world (Spray, 2015). The Vredefort Dome is situated in the Witwatersrand basin of the Kaapvaal Craton (Harris *et al.*, 2013). The Witwatersrand basin contains ~40% of the world's gold resources, which were made accessible for exploitation by the uplifting of the mineral rich geological structures that took place as a result of the meteorite impact (Reimold, 2014; Gibson & Reimold, 1999; Minter *et al.*, 1993). Apart from the economic value added by the Vredefort Dome, it is of great geological (e.g. large meteorite crater with inverted sedimentary structures), cultural and historical (e.g. stone age caves with remains of tools and humans, Khoi-San rock art, remnants of the Anglo-Boer War and old gold mines), conservational (e.g. diverse indigenous plant, animal and bird species, as well as water quality associated with Vaal River) and aesthetic (e.g. providing unique scenery with ecotourism opportunities) value in South Africa (UNESCO, 2015). Notwithstanding the national and international importance of the Vredefort Dome, currently no air quality data is available for this region. The recently compiled management plan, as required by the UNESCO declaration, also highlighted this knowledge gap (Engelbrecht, 2013). However,

currently it is not financially feasible to establish a state-of-the-art air quality monitoring station in this area. In order to partially address this knowledge gap, air masses that had passed over the Vredefort Dome were isolated and analysed in this study to provide an indication of the air quality over it. It is likely that the air quality in the Dome will be affected by the nearby declared priority areas, i.e. the Vaal Triangle Airshed Priority Area (VTAPA) (SA, 2006), the Highveld Priority Area (HPA) (SA, 2007) and the Waterberg Priority Area (WPA) (SA, 2012), which are well known for high levels of atmospheric pollution due to various anthropogenic activities. Furthermore, the Vredefort Dome could also be impacted by air masses passing over the Johannesburg-Pretoria conurbation (Lourens *et al.*, 2012).

1.2. Objectives

The general aim of the study was to characterise air masses and determine proxies for air quality in the Vredefort Dome and to compare these proxies with the relevant ambient air quality standards.

For this general aim, the specific objectives were:

i) Identifying back trajectories passing over the Vredefort Dome;

ii) Linking *in situ* atmospheric measurements of pollutant species conducted at the Welgegund monitoring station with the identified back trajectories;

iii) Comparing the measured pollutant concentrations that were linked with the appropriate back trajectory arrival times with National Ambient Air Quality Standards (NAAQS);

iv) Identifying possible trends in pollutant concentrations and relate these to possible sources; and

v) Presenting an assessment of the air quality over the Vredefort Dome based on the above-mentioned air quality proxies indicating what interventions are required in future.

Chapter 2

Literature survey

2.1. Air pollution

Air pollution can be defined as air containing gaseous, liquid or solid particles in sufficient concentrations, which can be harmful to human/animal health, welfare or comfort, as well as causing damage to materials and plants (Business Dictionary, 2015).

The earth's atmosphere consists of five layers in which the pressure and temperature change with altitude (Atkinson, 2000), i.e. the troposphere, stratosphere, mesosphere, thermosphere and the exosphere. The troposphere is the layer closest to the earth and is most significant for living organisms and meteorological events. The height of the troposphere is at the widest ~16 km and it contains 78.09% nitrogen (N_2), 20.95% oxygen (O_2), 0.93% argon (Ar), 0.03% carbon dioxide (CO_2), varying amounts of water (H_2O) vapour (depending on the temperature and altitude) and small amounts of other gases (Lourens, 2008; Connell, 2005; Atkinson, 2000). A majority of chemical species are emitted into the tropospheric layer from the surface, which undergo various chemical and physical transformations (Monks & Leigh, 2009).

Air pollution influences the troposphere and stratosphere differently. The earth-atmosphere radiation budget and the influence of gas species can be considered, with stratospheric ozone (O_3) and tropospheric CO_2 as examples. Stratospheric O_3 protects the biosphere from ultraviolet (UV) radiation by absorbing short-wave solar radiation (Connell, 2005), whereas tropospheric CO_2 retains infrared radiation within the troposphere (Fishman, 2003), i.e. the

greenhouse effect. Measurements over the past decades show that stratospheric O_3 has decreased and tropospheric CO_2 has increased (Fishman, 2003). A decrease in O_3 will result in damage to biota on the ground, while an increase in CO_2 will lead to warming of the earth's surface (Fishman, 2003). Greenhouse gas concentrations (e.g. CO_2 and methane (CH_4)) have increased significantly since the pre-industrial era and have contributed to global climate change. These gases absorb and reemit thermal infrared radiation from the sun that causes the earth's temperature to increase (Connell, 2005). Should the greenhouse gas emissions continue, increases in long lasting changes, warming of the climatic system, and severe impacts on the ecosystem and humans can be expected. The fifth assessment of the Intergovernmental Panel on Climate Change (IPCC) reports that the atmosphere and ocean have warmed since the 1950s, the lower troposphere has warmed and the lower stratosphere has cooled; extreme temperature changes and climate change have widespread impacts on human and natural systems (IPCC, 2014).

In addition to climate change, air pollution also has an effect on general air quality and human health. Kampa and Castanas (2008) state that air pollutants, depending on the dose and time of exposure, can lead to diverse impacts on human health. The different effects of air pollution can range from nausea, skin irritation or asthma to serious health effects such as cancer, birth defects and reduced activity of the immune system (Kampa & Castanas, 2008).

2.1.1. Types of air pollutants

A large number of air pollutant species are present in the atmosphere. These species have different chemical compositions, sources, reaction properties, transformations, impacts on human/animal health and the environment, persistence in the environment, and abilities to be transported over long or short distances (Venter, 2011; Kampa & Castanas, 2008). Air pollutants are generally grouped into two categories, i.e. gaseous species and aerosols.

Gaseous species

Gaseous pollutants are organic and inorganic compounds (Kampa & Castanas, 2008). Volatile organic compounds (VOCs), methane (CH_4), non-methane hydrocarbons and halogenated organic species are examples of typical atmospheric organic compounds (Kampa & Castanas, 2008; Daly & Zannetti, 2007). The most important inorganic species are nitrogen oxide (NO), nitrogen dioxide (NO_2), nitrous oxide (N_2O), sulphur dioxide (SO_2), ozone (O_3) and carbon monoxide (CO) (Kampa & Castanas, 2008). Greenhouse gas species that contribute significantly to climate change include CO_2, CH_4, O_3, N_2O and halogenated hydrocarbons (Daly & Zannetti, 2007; Connell, 2005).

Aerosols

Atmospheric aerosols or particulate matter (PM) are small solid or liquid particles that are suspended in the atmosphere that differ in size, morphology, number and shape (Kampa & Castanas, 2008). Aerosol particles originate from a mixture of natural (e.g. dust storms, volcanoes, sea spray) and anthropogenic (e.g. open cast mines, household combustion and industry) sources (Laakso *et al.*, 2012; Vakkari *et al.*, 2011; Venter, 2011; Ross *et al.*, 2003; Jayaratne & Verma, 2001). These particles can be characterised according to their aerodynamic particle diameter, e.g. ultra-fine ($PM_{0.1}$, < 0.1 µm), fine (PM_1, 0.1 µm > 1 µm) and coarse particles ($PM_{2.5}$ and PM_{10}, > 1 µm) (Kampa & Castanas, 2008).

2.1.2. Pollutant sources

Pollutant species are further classified as primary and secondary pollutants. Pollutants can be directly emitted into the atmosphere that are termed primary pollutants (Daly & Zannetti, 2007), while secondary pollutants are formed in the atmosphere from primary pollutants (precursors). Examples of typical primary pollutants, presented by Dally and Zannetti (2007), include:

- CO, CO_2, CH_4 and VOCs;
- NO, N_2O and NH_3;
- hydrogen sulphide (H_2S) and SO_2;
- halogen compounds; and
- particulate matter.

Some of the above-mentioned species can also be secondary pollutants, e.g. CO_2 formed from CO oxidation, SO_2 formed from H_2S oxidation and less volatile VOCs formed from more volatile species. Typical secondary pollutants presented by Dally and Zannetti (2007) are:

- nitric acid (HNO_3) and NO_2 formed form NO;
- O_3 formed form photochemical reactions of VOCs and nitrogen oxides;
- HNO_3 droplets formed from NO_2;
- sulphuric acid (H_2SO_4) droplets formed from SO_2;
- nitrate (NO_3^-) and sulphate (SO_4^{2-}) aerosols formed from reactions between H_2SO_4 and HNO_3 droplets and ammonia (NH_3), respectively; and
- organic aerosols formed from VOCs in gas-to-particulate reactions.

Atmospheric pollutants can originate from natural or anthropogenic sources. Natural sources include vegetation, soil surfaces, ocean and other aqueous surfaces, volcanic eruptions, dust storms, decompositions of animal and plant material and sea spray from oceans (Williams & Baltensperger, 2009). Typical anthropogenic sources include the combustion of fossil fuels, household combustion, vehicle emissions, chemical and petrochemical industries, agricultural activities, mining activities and high temperature combustion processes (Williams & Baltensperger, 2009).

2.2. Selection of species studied

Since this study was in principle an air quality study, species related to the National Ambient Air Quality Standards (NAAQS) were specifically considered, as well as some ancillary species. The NAAQS will be discussed in greater detail in Paragraph 2.3.

2.2.1. Nitrogen oxides

The important atmospheric nitrogen-containing species (with the exception of N_2) are NO, NO_2, N_2O, NH_3 and HNO_3 (Seinfield & Pandis, 2006). These species are primarily emitted into the atmosphere from anthropogenic activities such as vehicular emissions, coal-fired power plants, household combustion and agricultural activities (EPA, 2015; Shallcross, 2009), as well as naturally from microbial activity in soil by the reduction and oxidation of nitrogen compounds, e.g. reduction of NO_3^- and oxidation of NH_4^+ (Smith, 1982; Robinson & Robbins, 1970). The total nitrogen oxides, NO_x, (NO + NO_2), are approximately 30 % of the global budget (Monks & Leigh, 2009; Fabian & Pruchniewicz, 1977). NO_2 is the most prominent nitrogen-containing species and is emitted along with NO from combustion activities (Seinfield & Pandis, 2006). In urban areas, the highest NO_2 concentrations are found in the morning and late afternoon due to increasing motor vehicle activities (Lourens *et al.*, 2012; Venter *et al.*, 2012). South Africa is well known for the NO_2 hotspot over the Highveld Priority Area, where coal-fired power stations and petrochemical plants are the major sources (Lourens *et al.*, 2011). NO_2 takes part in chemical reactions (photolysis) that can lead to the formation of tropospheric O_3 (Connell, 2005). NO_2 can be regarded as a precursor for all the chemistry occurring in the atmosphere, if the photolysis of O_3 is considered the start of tropospheric chemistry (Pienaar & Helas, 1996). Once NO or NO_2 is released in the atmosphere, it undergoes a series of reactions (Venter, 2011; Shallcross, 2009; Atkinson, 2000) to form O_3.

$$NO + O_3 \rightarrow NO_2 + O_2 \quad 2.1$$

$$NO_2 + h\nu \rightarrow NO + O(^3P) \quad 2.2$$

$$O(^3P) + O_2 + M \rightarrow O_3 + M \ (M = N_2 \text{ or } O_2) \quad 2.3$$

These reactions interconvert NO, NO_2 and O_3, as is indicated in Figure 2.1.

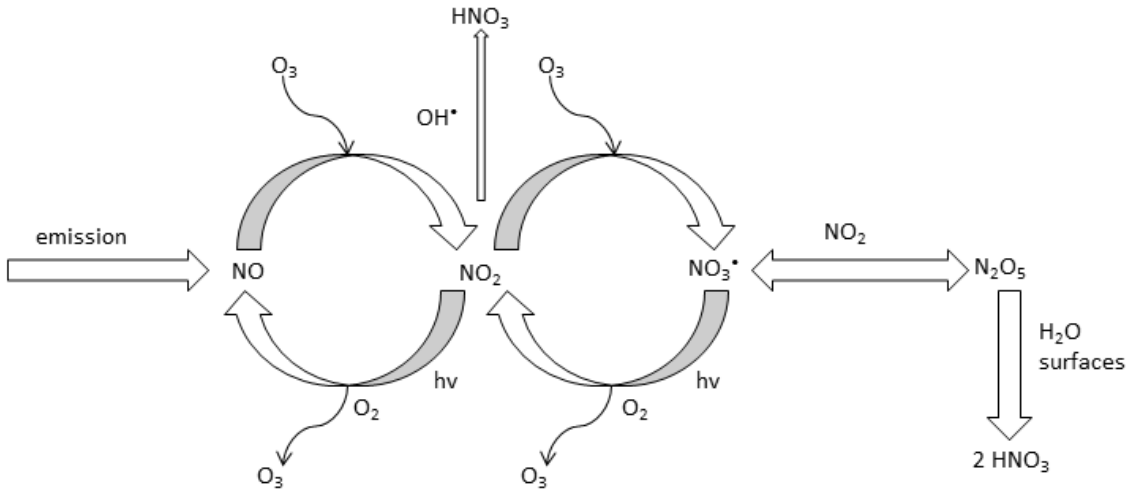

Figure 2.1 Tropospheric NO cycle (Atkinson, 2000)

The oxidation of NO_2 by O_3 can also lead to the formation of the nitrate radical, $NO_3^{\bullet}$ through the following reaction:

$$NO_2 + O_3 \rightarrow NO_3^{\bullet} + O_2 \quad 2.4$$

$NO_3^{\bullet}$, together with the hydroxyl radical ($HO^{\bullet}$) and O_3, is responsible for the majority of the oxidation reactions occurring in the troposphere. $NO_3^{\bullet}$ rapidly reacts (~ 5 seconds) with NO in the presence of sunlight to form NO again, as well as NO_2:

$$NO_3^{\bullet} + h\nu \rightarrow NO + O_2 \ (\sim 10\ \%) \quad 2.5$$

$$NO_3^{\bullet} + h\nu \rightarrow NO_2 + O(^3P) \ (\sim 90\ \%) \quad 2.6$$

Other important reactions of nitrogen oxides in the troposphere include:

$$HO^{\bullet} + NO \rightarrow HONO \quad 2.7$$

$HO^{\bullet} + NO_2 \rightarrow HNO_3$ 2.8

$NO_3^{\bullet} + NO_2 \rightarrow N_2O_5$ 2.9

$N_2O_5 + H_2O \rightarrow 2HNO_3$ 2.10

$NO_2 + NO + H_2O \rightarrow 2HNO_2$ 2.11

The reaction between $OH^{\bullet}$ and NO_2 is a major depleting chemical process for NO_x during the daytime (Atkinson, 2000). As indicated above, NO_x can also influence aerosol and wet deposition acidity, through the formation of nitrous acid (HNO_2) and HNO_3. Approximately 0.03% of CO_2 occurs in the troposphere, which in equilibrium with H_2O will result in precipitation with a pH of approximately 5.7 according to the Henry's Law (Connell, 2005). Additional acidity is usually ascribed to the presence of three inorganic acids, i.e. H_2SO_4, HNO_3 and HCl (Connell, 2005). Generally, H_2SO_4 dominates (which will be discussed in Paragraph 2.2.2) with less contribution from HNO_3 and comparatively low proportions of HCl (Connell, 2005).

2.2.2. Sulphur dioxide

The main atmospheric sulphur-containing compounds are SO_2, sulphur trioxide (SO_3), carbon disulphide (CS_2), carbonyl sulphide (OCS), H_2S and dimethyl sulphide (CH_3SCH_3) (Shallcross, 2009; Williams & Baltensperger, 2009). SO_2 is a highly reactive colourless gas emitted by anthropogenic fossil fuel burning (power plants) and other industrial processes (e.g. ore smelters and refineries) (EPA, 2015; Shallcross, 2009), as well as natural sources including volcanic eruptions and wildfires (EPA, 2009; Shallcross, 2009). In Figure 2.2, the global anthropogenic SO_2 trends as presented by various authors from 1900 up to 2000 are presented. Since the 19th century (1850), SO_2 emissions have increased rapidly due to increasing anthropogenic activities associated with the industrial revolution and power generation (Smith *et al.*, 2011). In the late 20th century, atmospheric SO_2 levels declined due

to the increase of global awareness of air quality that resulted in the introduction of technologies to remove SO_2 from industrial off-gas (Smith *et al.*, 2011).

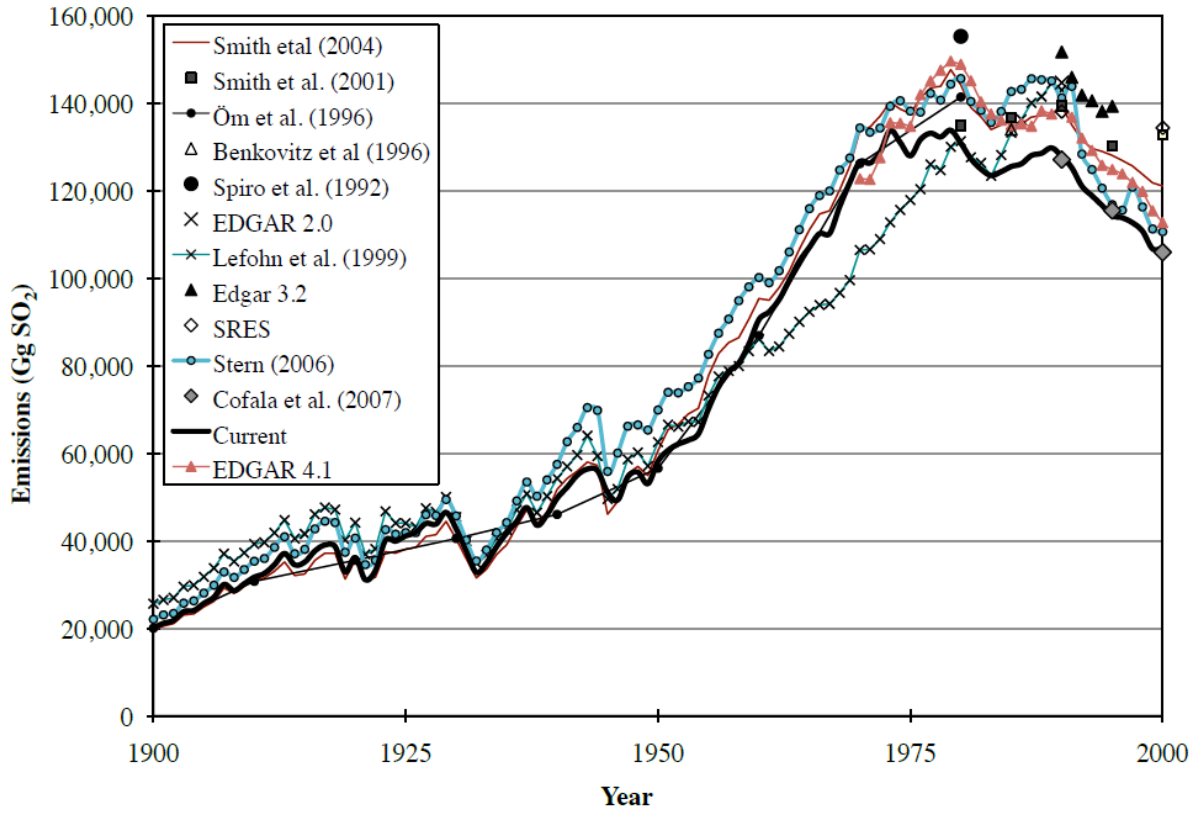

Figure 2.2 The global sulphur emission trends from several studies (Smith *et al.*, 2011)

The total SO_2 emissions in 2004 from southern Africa are presented in Figure 2.3 (Laakso *et al.*, 2012). The red star in this figure indicates the measurement location that Laakso *et al.* (2012) reported on and is not directly relevant to this study. As is evident from Figure 2.3, high SO_2 levels can be observed over the Mpumalanga Highveld (discussed in detail in Paragraph 2.3.), where there are industries associated with fossil fuel combustion such as coal-fired power stations and petrochemical industries (Lourens *et al.*, 2011).

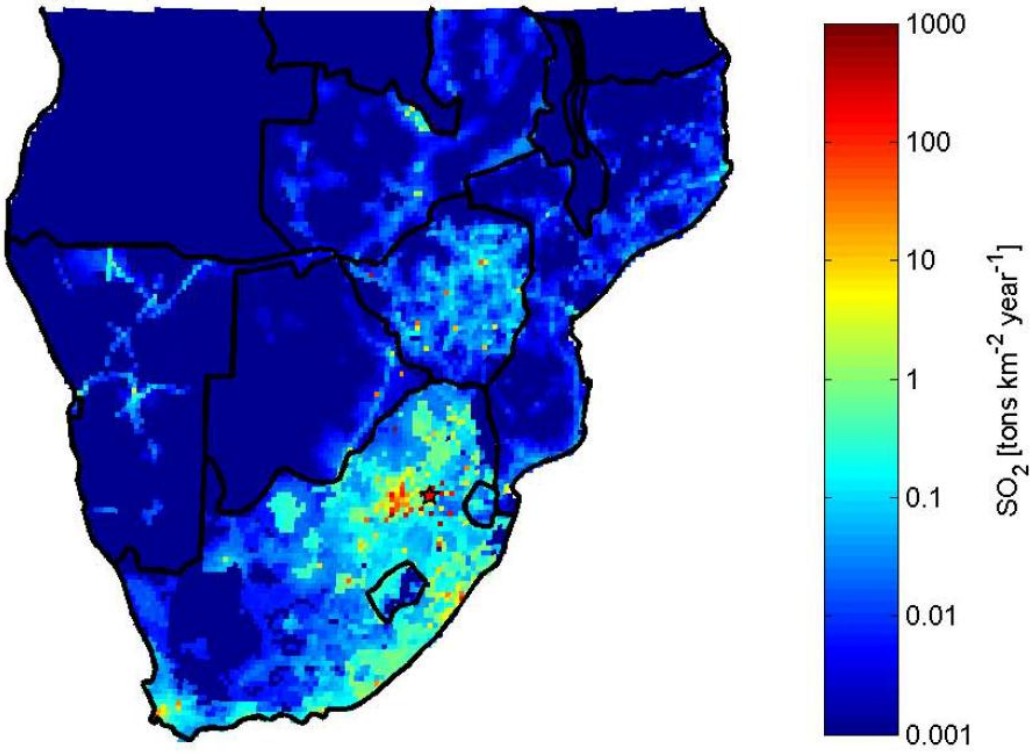

Figure 2.3 Total SO_2 emissions in southern Africa (2004) based on the SAFARI2000 emissions inventory (Laakso *et al.*, 2012; Fleming & van der Merwe, 2004)

Oxidation of SO_2 leads to the formation of H_2SO_4 aerosols in the atmosphere (Shallcross, 2009). In this process, SO_2 reacts with O_2 to form SO_3 (Seinfield & Pandis, 2006):

$$2SO_2 + O_2 \rightarrow 2SO_3 \qquad 2.12$$

The rate of the reaction between SO_2 and O_2 is very slow in atmospheric conditions. Therefore, SO_3 is more readily produced via the favourable $OH^{\bullet}$-radical abstraction reaction (Seinfield & Pandis, 2006):

$$OH^{\bullet} + SO_2 + A \rightarrow HOSO_2^{\bullet} + A \qquad 2.13$$

$$HOSO_2^{\bullet} + O_2 \rightarrow HO_2^{\bullet} + SO_3 \qquad 2.14$$

A reaction between SO_3 and H_2O then forms sulphuric acid (Seinfield & Pandis, 2006):

$$SO_3 + H_2O + A \rightarrow H_2SO_4 + A \qquad 2.15$$

(A = vibrational exchange of species)

Other sulphur-containing compounds can also form SO_2. For instance, H_2S undergoes a reaction with $OH^{\bullet}$ to form a $SH^{\bullet}$-radical and a series of other reactions to form SO_2 (Seinfield & Pandis, 2006):

$$H_2S + OH^{\bullet} \rightarrow SH^{\bullet} + H_2O \rightarrow SO_2 \quad 2.16$$

CH_3SCH_3 also undergoes reactions to form SO_2 (Seinfield & Pandis, 2006):

$$CH_3SCH_3 + HO^{\bullet} \rightarrow CH_3SCH_2O_2^{\bullet} \quad 2.17$$

$$CH_3SCH_2O_2^{\bullet} \rightarrow CH_3S^{\bullet} + HCHO \rightarrow SO_2 + CH_3 \quad 2.18$$

2.2.3. Ozone

Tropospheric O_3 is a secondary pollutant that is formed by photochemical reactions with NO_2 as indicated in Figure 2.1. Additionally, CO and VOCs can serve as precursor species for the formation of intermediates that lead to tropospheric O_3 formation (Jain, 2009; Jacob, 2000). Previous studies (Thompson *et al.*, 2014; Venter *et al.*, 2012; Lourens *et al.*, 2011; Josipovic *et al.*, 2010; Laakso *et al.*, 2008) have indicated that the interior of South Africa has elevated O_3 levels that are promoted by high concentrations of O_3 precursor emission, an abundance of sunlight and the recirculation of air masses of the interior that allows aging and photochemistry to take effect.

Figure 2.4 presents a schematic illustration of the chemical cycle of O_3, HO_x, NO_x and RO_2, which is a good example of the manner in which O_3 interacts with other species in the atmosphere (Jacob, 2000).

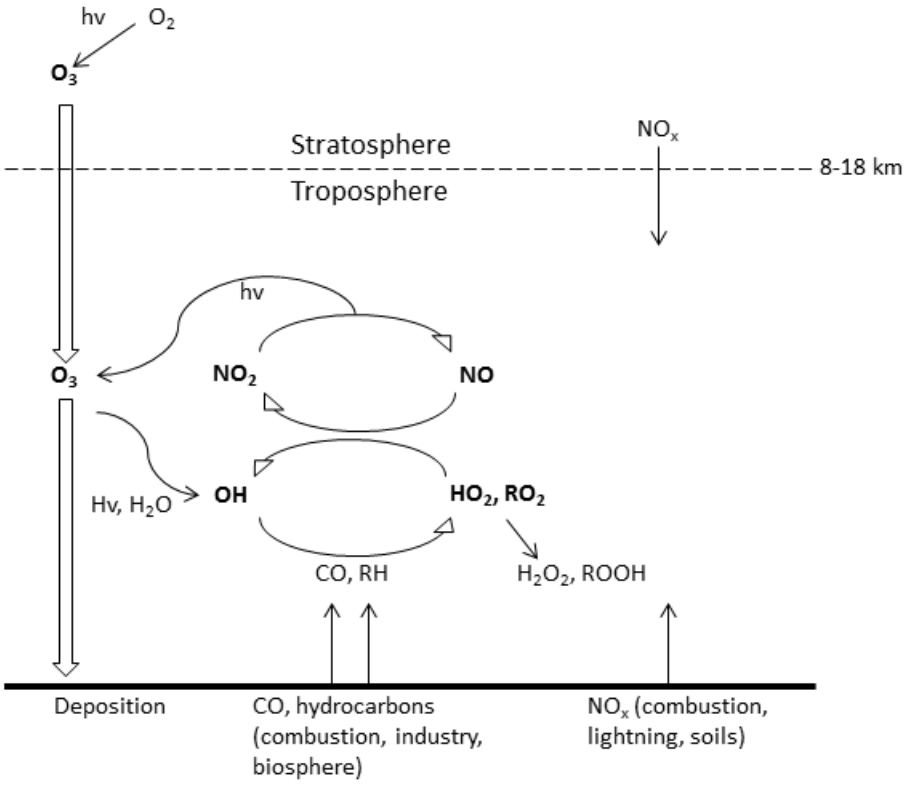

Figure 2.4 An illustration of the chemical cycle of O_3, HO_x, NO_x and RO_2. RO_2 refers to the mixture of organic peroxy radicals (Jacob, 2000)

Tropospheric O_3 production can be described as the HO_x-catalysed chain oxidation of CO and hydrocarbons in the presence of NO_x. As Seinfield and Pandis (2006) presented, photolysis of O_3 (at wavelengths < 319 nm) produces both ground state (O) and excited singlet ($O(^1D)$) oxygen atoms:

$$O_3 + hv \rightarrow O_2 + O(^1D) \quad 2.19$$

$$O(^1D) + M \rightarrow O(^3P) + M \ (M = N_2 \text{ or } O_2) \quad 2.20$$

$$O(^3P) + O_2 + M \rightarrow O_3 + M \quad 2.21$$

The singlet ($O(^1D)$) oxygen atom can react with water to form 2 $OH^{\bullet}$-radicals:

$$O(^1D) + H_2O \rightarrow 2HO^{\bullet} \quad 2.22$$

As indicated previously, $OH^{\bullet}$ is one of the most important chemicals in the atmosphere. It is short lived and reacts with most trace species present in the troposphere (Seinfield & Pandis,

2006). O_2 and O_3 are the most abundant oxidants in the troposphere, but are less reactive because of their large bond energies, which implies that $OH^{\bullet}$ is the primary oxidising species in the troposphere (Seinfield & Pandis, 2006).

2.2.4. Carbon monoxide

Carbon monoxide (CO) is the main pollutant emitted into the atmosphere due to incomplete combustion of carbon-based fuels (IPCC, 2013). In urban areas, motor vehicle emissions are the main pollutant source for CO and contribute approximately 70 % of CO (Fenger, 2009). In South Africa, CO is also emitted in large amounts from savannah and grassland fires in winter and early spring (Swap *et al.*, 2003; Jayaratne & Verma, 2001; Maenhaut *et al.*, 1996), as well as from household combustion in low income informal settlements (Venter *et al.*, 2012; Laakso *et al.*, 2008; Novelli, 2003).

The two main impacts associated with tropospheric CO are related to its toxicity (Kampa & Castanas, 2008; Ernst & Zibrak, 1998) and its contribution to O_3 formation (Connell, 2005). Photolysis of O_3 leads to the formation of $OH^{\bullet}$ that oxidises CO to form $HO_2^{\bullet}$-radicals in the troposphere that catalyse tropospheric O_3 formation (Seinfield & Pandis, 2006; Novelli, 2003):

$$OH^{\bullet} + CO + O_2 \rightarrow CO_2 + HO_2^{\bullet} \quad 2.23$$

$$HO_2^{\bullet} + NO \rightarrow NO_2 + OH^{\bullet} \quad 2.24$$

$$NO_2 + h\nu \rightarrow NO + O(^3P) \quad 2.25$$

$$O(^3P) + O_2 + M \rightarrow O_3 + M \quad 2.26$$

Novelli (2003), and references therein, indicated that trends in CO levels are expected to have an effect on climate through the regulation of $OH^{\bullet}$ concentrations, which affect the levels of several greenhouse gases. $HO_2^{\bullet}$-radicals produced through CO oxidation can lead to the formation of O_3 through a series of photochemical reactions in areas with high NO levels

(Novelli, 2003). If the NO concentration is low, O_3 may be destroyed by the $HO_2^{\bullet}$-radical produced by the oxidation of CO (Novelli, 2003):

$$O_3 + HO_2^{\bullet} \rightarrow 2O_2 + OH \qquad 2.27$$

2.2.5. Particulate matter

Atmospheric aerosols consist of a mixture of organic and inorganic compounds. They can differ in size ranges from a few nanometres to micrometres in diameter (Seinfield & Pandis, 2006). Tropospheric aerosols can contain NO_3^-, SO_4^{2-}, sodium (Na^+), chloride (Cl^-), ammonium (NH_4^{2+}), black (elemental) carbon (BC), organic compounds (OC), water and crustal elements (Seinfield & Pandis, 2006). The lifetime of aerosols can range from a few hours up to weeks, depending on the aerosol properties (e.g. size) and metrological conditions (Pöschl, 2005). Aerosols can be emitted from natural or anthropogenic sources. Primary aerosols can be from natural sources, e.g. volcanic eruptions, wind-blown dust, sea spray and biological materials, as well as from anthropogenic sources, e.g. industrial activities such as incomplete combustion of fossil fuels (Pöschl, 2005). Secondary aerosols are formed by gas-to-particle conversions in the atmosphere. Gaseous precursors lead to new particle formation by condensation and nucleation in the atmosphere (Pöschl, 2005). Recent studies (Gierens *et al.*, 2014; Hirsikko *et al.*, 2013; Vakkari *et al.*, 2013; Hirsikko *et al.*, 2012; Vakkari *et al.*, 2011; Laakso *et al.*, 2008) have indicated that the rate and frequency of new particle formation in South Africa are among the highest in the world.

Figure 2.5 illustrates that airborne aerosols can undergo chemical and physical transformations and interactions (Pöschl, 2005). Aerosols can change in composition, structure and size by coagulating with other particles, through chemical reactions, and by condensation of vapour species or evaporation that can become fog and cloud droplets through the activation in the presence of water supersaturation (Seinfield & Pandis, 2006;

Pöschl, 2005). They also affect the distribution and abundance of atmospheric trace gases by heterogeneous chemical reactions and other multiphase processes (Pöschl, 2005).

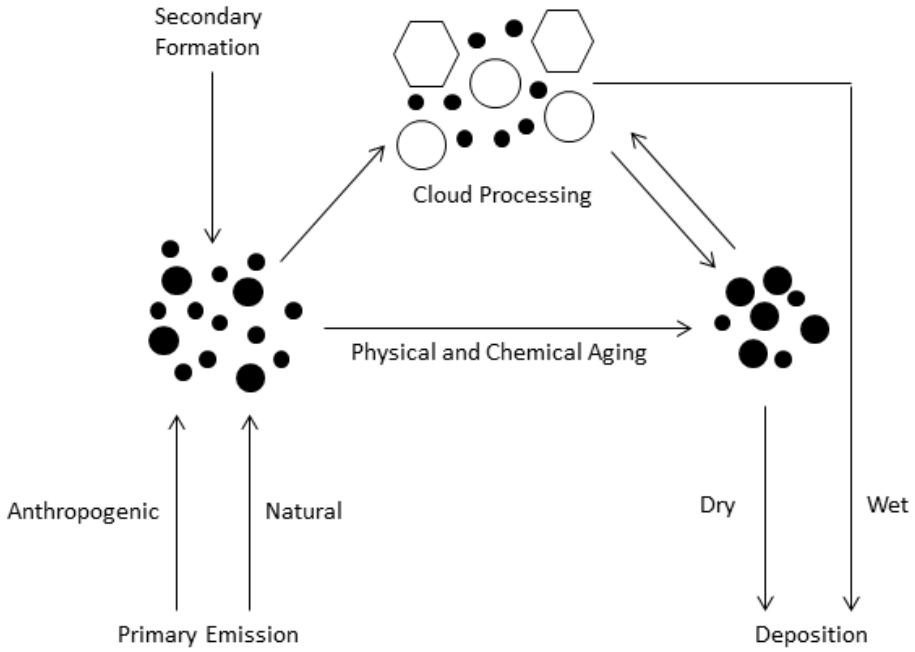

Figure 2.5 The cycle of atmospheric aerosols (Pöschl, 2005)

Depending on the size and chemical composition, aerosols can have health effects ranging from allergic diseases to respiratory and cardiovascular diseases (Pöschl, 2005; Bernstein *et al.*, 2004). Aerosol particles also have direct (scattering or absorption of solar radiation) and indirect (acting as cloud condensation nuclei, CCN, and mimicking the properties of clouds) radiative effects on the earth's climate system (Laakso *et al.*, 2012; Vakkari *et al.*, 2011; Penner *et al.*, 2001). Aerosol scattering has a cooling effect on the climate and makes the earth more reflective, while aerosol absorption has a warming effect on the climate (IPCC, 2014). The fifth assessment report of the IPCC indicated that most studies agree that anthropogenic aerosols' net radiative effect is cooling the earth.

Pöschl (2005) described how clouds form from the condensation of water vapour on pre-existing aerosol particles (CNN and ice nuclei, IN). Atmospheric aerosols can be removed by two mechanisms, i.e. wet deposition and dry deposition (Figure 2.5) (Seinfield & Pandis,

2006). Wet deposition takes place when modified aerosol particles are released from evaporating cloud droplets or ice crystals during the formation of precipitation that reaches the earth's surface (Pöschl, 2005). Aerosol particles that reach the earth's surface without precipitation, but by diffusion, convective transport and adhesion, are called dry deposition (Pöschl, 2005).

2.2.6. Black carbon (BC)

BC is a primary aerosol that is directly emitted from incomplete combustion of fossil fuels, biomass burning and pyrolysis of carbonaceous matter (IPCC, 2007). BC contributions to the global budget are estimated to be ~ 42 % from biomass burning, ~ 38 % from fossil fuels and ~ 20 % from biofuel (Sahu *et al.*, 2011; Bond *et al.*, 2004). Due to BC's graphitic type structure, it can absorb radiation in visible, near UV and near infrared regions (Sahu *et al.*, 2011; Rosen *et al.*, 1978). Figure 2.6 presents typical BC sources and the role they play in the atmosphere (Bond *et al.*, 2013). The IPCC's fourth assessment report and references therein indicated that BC particles can reduce solar radiation from reaching the earth's surface and tend to warm the atmosphere at regional scales affecting the vertical temperature profile and hydrological cycle. Deposited BC particles can accelerate melting of snow, glaciers and sea ice by reducing the surface albedo, which makes the arctic climate vulnerable (McConnel *et al.*, 2007; Jacobson, 2001). BC gets mixed with other particles/gases in the atmosphere, which can alter it (Sahu *et al.*, 2011; Lazaridis, 2008; Rosen *et al.*, 1978). When SO_4^{2-} and less volatile organic compounds are deposited as a coating on BC particles, it can enhance absorption and/or scattering, and additionally activate it as CCN (IPCC, 2014). Most atmospheric BC particles comprises mainly of fine particles (90 % in the $PM_{2.5}$ fraction) (Sahu *et al.*, 2011). Similar to other aerosols, BC can act as CCN that affects the cloud cover and -lifetime, which also may have warming and cooling effects on clouds (Koch & Del Genio, 2010).

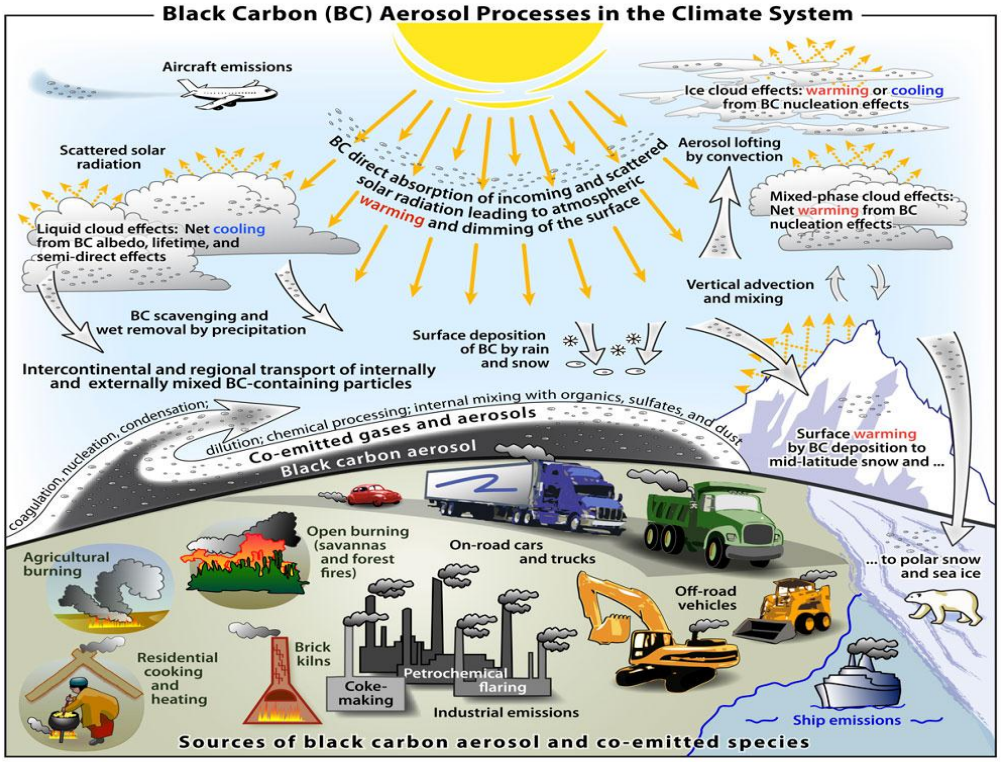

Figure 2.6 A schematic overview of the interactions between BC and the earth's system (Bond *et al.*, 2013)

2.3. *Air quality standards and priority areas*

In order to prevent direct and indirect adverse effects on human health and the environment associated with atmospheric pollution, it is necessary to measure and report air quality on a local, regional and global scale. State and federal agencies (e.g. World Health Organisation (WHO) and the Environmental Protection Agency (EPA)) have developed guidelines and standards to improve air quality worldwide and reduce harmful emissions in order to protect the public.

Air quality measurements and the improvement thereof are considered priorities in developed countries. In developing countries, less emphasis is placed on environmental problems. South Africa can be regarded as a developing country with elements of a developed country. Due to biomass burning emissions (Swap *et al.*, 2003) and the NO_2 (and SO_2 to a less degree)

hotspot over the Highveld (Lourens *et al.*, 2011), South Africa is considered as a globally important source region for atmospheric pollutants.

In 2009, South Africa established the National Ambient Air Quality Standards (NAAQS) according to the National Environmental Management: Air Quality Act, 2004 (SA, 2009). The NAAQS regards SO_2, NO_2, O_3, CO, benzene (C_6H_6), lead (Pb) and PM_{10} (particulate matter with an aerodynamic diameter less than or equal to 10 µm) as criteria pollutants. These species were selected since they were regarded as the most important and most commonly monitored in the atmosphere due to their influence on human health and the environment. In Table 2.1, the NAAQS and associated limits are presented.

Table 2.1 NAAQS established according to the National Environmental Management: Air Quality Act, 2004 (SA, 2009)

Averaging period	Concentration	Frequency of exceedance	Compliance date
National Ambient Air Quality Standards for sulphur dioxide (SO_2)			
10 minutes	500µg/m^3 (191 ppb)	526	Immediate
1 hour	350µg/m^3 (134 ppb)	88	Immediate
24 hours	125µg/m^3 (48 ppb)	4	Immediate
1 year	50µg/m^3 (19 ppb)	0	Immediate
The reference method for the analysis of sulphur dioxide shall be ISO 6767			
National Ambient Air Quality Standards for nitrogen dioxide (NO_2)			
1 hour	200µg/m^3 (106 ppb)	88	Immediate
1 year	40µg/m^3 (21 ppb)	0	Immediate
The reference method for the analysis of nitrogen dioxide shall be ISO 7996			
National Ambient Air Quality Standards for particulate matter (PM_{10})			
24 hours	120µg/m^3	4	Immediate – 31 December 2014

24 hours	75µg/m^3	4	1 January 2015
1 year	50µg/m^3	0	Immediate - 31 December 2014
1 year	40µg/m^3	0	1 January 2015
The reference method for the determination of the particulate matter fraction of suspended particulate matter shall be EN 12341			
National Ambient Air Quality Standards for ozone (O_3)			
8 hours (running**)**	120µg/m^3 (61 ppb)	11	Immediate
The reference method for the analysis of ozone shall be UV photometric method as described in SANS 13964			
National Ambient Air Quality Standards for benzene (C_6H_6)			
1 year	10µg/m^3 (3.2 ppb)	0	Immediate – 31 December 2014
1 year	5µg/m^3 (1.6 ppb)	0	1 January 2015
The reference methods for the sampling and analysis of benzene shall either be EPA compendium method TO-14 A or method TO-17			
National Ambient Air Quality Standards for lead (Pb)			
1 year	0.5µg/m^3	0	Immediate
The reference method for the analysis of lead shall be ISO 9855			
National Ambient Air Quality Standards for carbon monoxide (CO)			
1 hour	30µg/m^3 (26 ppm)	88	Immediate
8 hour (calculated on 1-hourly averages)	10µg/m^3 (8.7 ppm)	11	Immediate
The reference method for analysis of carbon monoxide shall be ISO 4224			

South African legislation also makes provision for recognising areas with high levels of air pollution, which are termed priority areas. These areas have elevated pollution concentrations that frequently exceed the limit values for criteria pollutants in the NAAQS. Three priority areas have been declared by the South African government, i.e. the Vaal Triangle Airshed Priority Area (VTAPA) (SA, 2006), the Highveld Priority Area (HPA) (SA, 2007) and the

Waterberg Priority Area (WPA) (SA, 2012) to improve air quality in these regions. The VTAPA was the first priority area to be declared in 2006. This area mostly contains large petrochemical operations, pyro-metallurgical smelters, a coal-fired power station, mining operations and domestic fuel burning, with none of the afore-mentioned industrial sources removing sulphur- and nitrogen-containing compounds from their off-gas (de-SO_x and de-NO_x) (SA, 2009). The HPA was declared in 2007. The large emission sources of this area include eleven coal-fired power stations (responsible for the majority of electricity generation in South Africa), several pyro-metallurgical smelters, open cast mining, a very large petrochemical operation and domestic fuel burning, again all industrial sources without de-SO_x and de-NO_x technologies (Laakso *et al.*, 2012; SA, 2011; Lourens *et al.*, 2011). An NO_2 hotspot, of which the tropospheric NO_2 column density is comparable to some of the most polluted areas in the world, is clearly visible over this area from satellite observations (Lourens *et al.*, 2011). The WPA was declared in 2012. This area contains a large fraction of the South African mineral assets. In this area, eleven pyrometallurgical smelters occur within approximately 55 km radius, two large coal-fired power stations and domestic fuel burning activities (Van Zyl *et al.*, 2014; Hirsikko *et al.*, 2012). The platinum group metals (PGMs) smelters in this area apply de-SO_x technology (e.g. Westcott *et al.*, 2007), but not de-NO_x, while none of the other smelters (e.g. ferrochrome and ferrovanadium) and the coal-fired power stations apply de-SO_x or de-NO_x technologies.

SO_2, NO_2, O_3, CO and PM_{10} are the criteria pollutants that were selected for monitoring in this study, since these species were already monitored at the Welgegund research station that will be introduced later (Chapter 3, Paragraph 3.1).

2.4. The Vredefort Dome World Heritage Site

The Vredefort Dome is of great geological, cultural, historical, conservational and aesthetic value in South Africa. It contains historical evidence of former human activities, such as Stone Age caves with remains of tools and humans, Khoi-San rock art, remnants of the Anglo-Boer War and old gold mines, all of which contribute to the South African cultural heritage (UNESCO, 2015). The Vaal River, one of the longest (1 105 km) rivers in South Africa and tributary of the Orange River, flows through the Dome and is the key water source for Johannesburg and east-central South Africa, providing unique scenery and aesthetic value within the Dome. It is also rich in diverse indigenous plants (more than 99 plant species), animals (more than 50 small mammal species) and birds (more than 200 bird species) (UNESCO, 2015). In Figure 2.7, the hills within the Vredefort Dome with indigenous plant species and Vaal River can be observed that contribute to its unique scenery.

Figure 2.7 A scenic picture of the Vredefort Dome hills, indigenous plant species and flowing Vaal River (http://www.southafricatravels.com/103/the-vredefort-dome/)

In 2007, the Vredefort Dome was proclaimed to be South Africa's seventh world heritage site and was added to the United Nations Educational, Scientific and Cultural Organization (UNESCO) world heritage site list (UNESCO, 2015; SA, 2007). Examples of other national world heritage sites in South Africa are Robben Island, the Cape Floral Regions and the Fossil Hominid Site of South Africa, while international sites include the Grand Canyon National Park in the United States of America (USA) and Stonehenge in the United Kingdom (UK) (UNESCO, 2015). According to the Online Oxford English Dictionary (2015), a world heritage site is a man or natural made structure, area or site of outstanding universal value and is therefore worthy of protection. The World Heritage Committee inscribes the protection of the site in the World Heritage List in terms of the World Heritage Convention (an organisation of UNESCO) (Online Oxford English Dictionary, 2015). There are currently approximately 150 known meteorite impact structures on earth, all between the size of <1 to > 250 km in diameter (Reimold & Gibson, 1996; Grieve *et al.*, 1995). Among two other large meteorite impact structures, i.e. the Sudbury impact structure (diameter of ~130 km) in Canada (UNESCO, 2015; Deutsch *et al.*, 1995) and the Chicxulub impact structure (diameter of ~150 km) in Mexico (UNESCO, 2015; Earth Impact Database, 2011; French, 1998), the Vredefort Dome (diameter ~160 km) in South Africa is the world's largest, one of the oldest (~ 2023 million years) and one of the most visible meteorite impact structures in the world (UNESCO, 2015; Brink *et al.*, 2000; Reimold & Gibson, 1996). Although the Vredefort Dome has been exposed to thousands of years of erosion and most of it is covered by sedimentary rocks of the Karoo Supergroup, its features are still visible today, which further adds to its rare and unique qualities (UNESCO, 2015).

The Vredefort Dome World Heritage Site is ~ 120 km south-west from Johannesburg and is located on the boundary between the North West Province and the Free State Province. The heritage property, including the outcrops that indicate meteorite impact structure phenomena,

has a total size of 30 111 ha and consists of the main area and three geological outcrops (UNESCO, 2015; SA, 2007). The main area has a total surface area of 30 108 ha and the three geological (outcrop) satellite sites are 1 ha each (UNESCO, 2015). The Vredefort Dome region is protected against external developments by the implementation of a 5 km buffer zone around the property area, which makes the property area a total of 44 530 ha (UNESCO, 2015). It consists of 146 privately owned properties (farms), of which 89 are located in the North West Province and 57 in the Free State Province, while approximately 600 ha are state owned (UNESCO, 2015). Land use on the privately owned properties includes agriculture, game farming, resort accommodation, youth camps, team building activities and tourism activities (UNESCO, 2015).

The Vredefort Dome is situated in the Witwatersrand basin of the Kaapvaal Craton (Harris *et al.*, 2013). The Gauteng province of South Africa is known as the world's largest gold-producing province (Harris *et al.*, 2013). The Witwatersrand basin that extends as far as Johannesburg in the north-east and Welkom in the south-east is the remnant of the outer parts of the impact structure and contains ~40% of the world's gold resources (Reimold, 2014; Gibson & Reimold, 1999; Minter *et al.*, 1993). A geological cross section in the central area of the Vredefort Dome illustrates that deep situated rocks, i.e. the Witwatersrand basin, have been uplifted by the meteorite impact that exposed the mineral rich geological structures for exploitation and contributes to our knowledge of the earth's inner structure (Reimold, 2014).

Chapter 3

Experimental procedures

3.1. Measuring site location

Measurements were conducted at the Welgegund monitoring station (www.welgegund.org) (26°34'10"S, 26°56'21"E, 1480 m above mean sea level) situated ~100 km west of Johannesburg and 25 km north-west from Potchefstroom in the North West Province of South Africa. The location of the Welgegund monitoring station (black star) is presented in Figure 3.1. The station is located on a commercial farm and surrounded by grassland savannah with moderate temperatures and dry winters with precipitation occurring mainly in the spring and summer seasons (Jaars *et al.*, 2014; Tiitta *et al.*, 2014; Beukes *et al.*, 2013). A more detailed description of the Welgegund measuring station is presented in previous papers (Beukes *et al.*, 2015; Booyens *et al.*, 2015; Kuik *et al.*, 2015; Jaars *et al.*, 2014; Tiitta *et al.*, 2014; Vakkari *et al.*, 2014; Beukes *et al.*, 2013). The Welgegund monitoring station is considered a regional background site with no major nearby direct impacts of anthropogenic pollution sources. Relatively clean background air originates from the western sector (from north to south-east) that contains no major point sources (Jaars *et al.*, 2014; Tiitta *et al.*, 2014; Beukes *et al.*, 2013). However, pollution plumes can be observed from the declared priority areas (Paragraph 2.3) and Johannesburg-Pretoria (Jhb-Pta) megacity (Jaars *et al.*, 2014; Tiitta *et al.*, 2014; Beukes *et al.*, 2013; Lourens *et al.*, 2012), as well as from the regional savannah and grassland fires that occur in the dry season in South Africa (Vakkari *et al.*, 2014; Tiitta *et al.*, 2014; Jayaratne & Verma, 2001). The Welgegund measurement site is ~60 km from the

centre of the Vredefort Dome World Heritage Site and is most likely the closest comprehensively equipped long-term continuously operating atmospheric monitoring station.

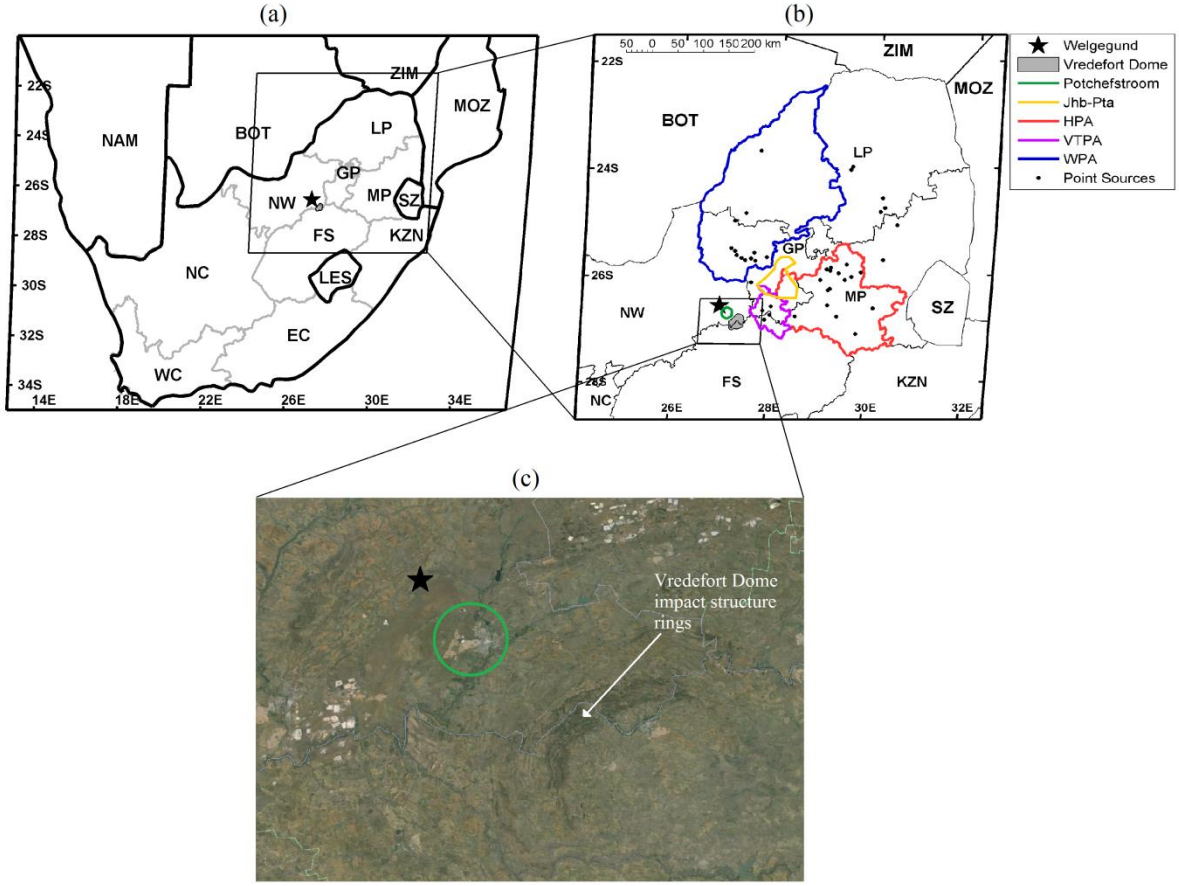

Figure 3.1: (a) The location of the Vredefort Dome within a regional context. (Countries: Nam – Namibia, Bot – Botswana, Zim – Zimbabwe, Moz – Mozambique, Sz – Swaziland, Les – Lesotho, South African provinces: WC – Western Cape, EC – Eastern Cape, NC – Northern Cape, FS – Free State, KZN – KwaZulu-Natal, NW – North West, MP – Mpumalanga, LP – Limpopo Province). (b) The positioning of the Welgegund monitoring station and spatial extent of the declared priority areas and the Jhb-Pta megacity, as well as very large point sources in the South African interior are indicated on the zoomed-in map. (c) A Google Earth image of the area clearly indicating the rings that form part of the Vredefort Dome impact structure.

3.2. Sampling methods and data processing

Atmospheric measurements were conducted at Welgegund for a sampling period from 1 June 2010 to 28 February 2014, which were only interrupted when instruments were serviced or calibrated when general maintenance was performed and during power failures. The Welgegund monitoring station hosts a comprehensive set of continuous measurements as presented in previous papers (Beukes *et al.*, 2015; Booyens *et al.*, 2015; Jaars *et al.*, 2014; Tiitta *et al.*, 2014; Vakkari *et al.*, 2014; Beukes *et al.*, 2013).

The Welgegund monitoring station was visited at least once a week for maintenance. This weekly maintenance consisted of inspection and adjustment of instrument flows, inlet cleaning and other *ad hoc* procedures. Once a month, the filters on the gaseous instruments were changed, radiation sensors were cleaned and the PM_{10} measurement equipment was calibrated. Comprehensive gas calibrations were conducted quarterly. For quality assurance, the data was downloaded and visually inspected every day. Additional site visits were arranged if irregularities appeared in the data or in diagnostic data (e.g. cell temperatures and flows). An electronic diary, recording all site visits and actions taken, was also kept.

The raw high resolution atmospheric 1-min data from the site was processed to account for power failures, recovery periods after power failures, as well as calibrations or maintenance of instruments. The data was visualised and corrected with a fit-for-purpose MATLAB program set based on diary entries and periods of uncertain data quality were automatically eliminated. The data was then automatically corrected based on calibrations (zero and span), as well as flow checks. Finally, the data was visually inspected. After the afore-mentioned quality assurance procedures were applied, the 1-min high resolution data was converted to 15 min averages. A 15 min average was only calculated if at least two thirds of the 1-min data were available. The conversion of measured gaseous mixing ratio (in parts per billion by volume, ppbv) to $\mu g/m^3$ was conducted at standard temperature and pressure (0 °C and 101.3

kPa). All particle concentrations were also converted to standard temperature and pressure conditions.

3.3. Analysis of air mass histories and associating with in situ measurements

HYSPLIT 4.8 (HYbrid Single-Particle Lagrangian Intergrated Trajectory) was used to calculate 96-hour back trajectories, arriving hourly, throughout the entire measurement period with an arrival height of 100 m (Air Resources Laboratory, National Oceanic and Atmospheric Administration, 2015). An arrival height of 100 m was chosen because the orography in HYSPLIT is not very well defined, and therefore lower arrival heights could result in increased error margins on individual trajectory calculations. Considering the above, 24-hourly arriving back trajectories for each day were obtained for the entire sampling period.

In order to obtain a statistical overview of air mass history, overlay back trajectory maps were generated. This was performed by superimposing individual back trajectories generated in HYSPLIT with a fit-for-purpose MATLAB script on maps that were divided into 0.2 X 0.2°grid cells (Venter *et al.*, 2012). Colour was used to indicate the percentage of trajectory passing over specific grid cells, with red and dark blue representing the highest and lowest percentages, respectively. Additionally, individual back trajectories were sorted to obtain trajectories that had passed over the Vredefort Dome area before arriving at Welgegund, but did not pass over significant sources after passing over the Dome. This was accomplished by first defining polygons representing the surface areas of the proclaimed Vredefort Dome area, the city of Potchefstroom that lies in between the Dome and Welgegund, as well as the surface area that included the Jhb-Pta megacity and all the very large point sources (e.g. coal-fired power stations, metallurgical smelters and large

petrochemical operations) occurring within the previously mentioned priority areas. Individual back trajectories were then sorted to find those that had passed over the Vredefort Dome before arriving at Welgegund, but that did not pass over either Potchefstroom or the priority areas after passing over the Dome. Figure 3.2a indicates an example of an appropriate trajectory, while Figures 3.2b and 3.2c indicate examples of trajectories that had passed over the Vredefort Dome that subsequently passed over either the large point source region or over Potchefstroom, respectively, before arriving at Welgegund.

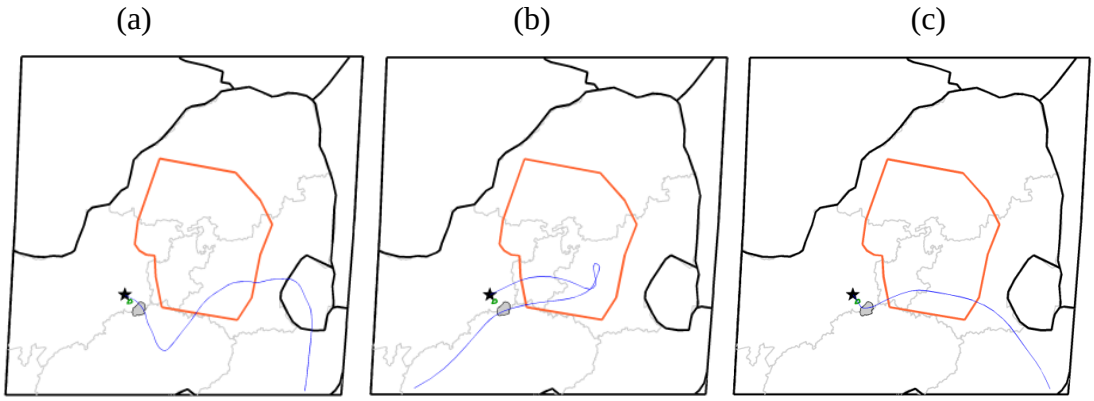

Figure 3.2: (a) An example of a back trajectory that had passed over the Vredefort Dome before arriving at Welgegund, but that did not pass over either Potchefstroom or the LPS region after passing over the Dome. (b) and (c) are examples of the back trajectories that had passed over the Vredefort Dome, but that did not comply with the selection criteria indicated in (a)

The 15 min average data of the *in situ* pollutant species measured at Welgegund was linked to the air mass history by associating every selected hourly arriving back trajectory, with the two 15 min average before the hourly arrival time, as well as the two 15 min averages after the hourly back trajectory arrival time. This implies that each selected back trajectory was associated with four 15 min averages of the *in situ* measurements.

3.4. Sampling equipment

3.4.1. Meteorology

The ambient temperature and relative humidity were measured with a Rotronic MP 101A instrument, while wind speed and direction were measured with a Vector A101ML and A200/L, respectively. Precipitation was measured with a tip bucket rain intensity meter (Vaisela QMR102).

3.4.2. NOx

NO_x measurements were conducted with a Teledyne 200AU $NO/NO_2/NO_x$ analyser. The instrument measures the concentration of NO and NO_x from which NO_2 is calculated. It has an upper detection limit of 2 000 ppb and measures at intervals of 1 ppb. As described in the manual, the analyser measures the light intensity of the chemiluminescent gas phase reaction between NO and O_3. The reaction follows:

$$NO + O_3 \rightarrow NO_2^* + O_2 \quad 3.1$$

$$NO_2^* \rightarrow NO_2 + hv \quad 3.2$$

Electronically excited NO_2 forms from the reaction between NO and O_3 where the excited molecules (Equation 3.1) return to the ground state and the excess energy is released (Equation 3.2) (API, 1999). The light intensity is directly proportional to the NO concentration. The analyser samples the gas stream and measures the NO concentration by digitising the signal from the analyser's photomultiplier tube (PMT) (API, 1999). A valve then routes the sample stream through a converter containing heated (315°C) molybdenum (Mo) to reduce any NO_x present to NO (API, 1999). The reaction follows:

$$3NO_x + Mo \rightarrow 3NO + MoO_3 \quad 3.3$$

The analyser then measures the total NO_x concentration. The NO_2 concentration is calculated by automatically subtracting NO concentrations from NO_x concentration values (API, 1999).

The instrument then measures sample gas that has been mixed with O_3 outside of the reaction cell. This pre-reactor allows the measurement of any hydrocarbon interferences present in the sample gas stream. The three concentration results NO, NO_x, and NO_2 are then further processed and stored by the computer yielding several instantaneous and long-term averages of all three components (API, 1999).

3.4.3. SO_2

A Thermo-Electron 43S SO_2 analyser from Thermo Environmental Instruments Inc. was used to measure ambient SO_2 concentrations. The detection limit is 0.1 ppb and a flow rate of 0.5 l/m was maintained. The analyser provides continuous, real-time measurements of ambient SO_2 by pulsed fluorescence. In this technique, the SO_2 molecules absorb fluorescent energy, producing an electronically excited SO_2 molecule with a known spectral decay rate. As the excited SO_2 molecules state decay, the molecules emit characteristic radiation. A photo multiplier tube detects the fluorescence emitted and the signal is proportionally converted to an electronic output signal. The signal is then filtered and amplified to appropriate display levels. There are many wavelengths that can be used; however, for this analyser, a wavelength of 230-190 nm was utilised. This wavelength has the lowest signal noise, is the most stable and is not influenced by any other pollutant species (Thermo Environmental Instruments, 1989).

3.4.4. O_3

The Environment SA 41M analyser was used to measure O_3. The detection is based on the absorption of ultraviolet light (253.7 nm) by O_3. This instrument allows for continuous operation for long periods and has a detection limit of 1 ppb with a sample flow rate of 1.6l/min (Environment, 1999). A full measurement cycle consists of the following several steps. The gas passes through the O_3 selective filter and ventilation in the measurement chamber occurs. UV energy is measured through the chamber without the O_3 sample. The gas

is then routed to a block made up of a three-way solenoid valve. The switching of the solenoid valve allows the sample to pass directly into the measurement chamber and UV energy is measured through the chamber with the O_3 sample where the O_3 molecules selectively absorb the UV rays. The amount of UV absorbed by the O_3 molecules is in proportion to the concentration (Environment, 1999).

3.4.5. CO

CO was measured with a Horiba APMA-360 analyser. It uses cross-flow modulated non-dispersive mono-beam infrared absorption to measure CO that eliminates the need for optical adjustments. This ensures sensitive and stable measurements. Sample air and reference air are alternately sent to a measurement cell by three-way solenoid valve operating at a constant duty cycle at a constant flow rate. The infrared beam passes through the gas in the measurement cell. CO concentration is calculated by subtracting the sample air and reference air concentrations. The reference gas is generated by oxidising the CO to CO_2 in the sample air (Venter, 2011). This prevents the interference of other elements, resulting in extremely accurate measurements. Energy absorbed by the detector displaces the membrane in the cell. The displacement is converted into an electrical signal, amplified and read processor (South Coast Air Quality Management District, 2012).

3.4.6. PM_{10}

A synchronised hybrid ambient real-time particulate (SHARP), model 5030, analyser was used to determine the total mass of atmospheric PM_{10} particles. The analyser consists of a C^{14} source, detector and a light scattering Nephelometer. The SHARP utilises proprietary digital filtering to continuously mass calibrate the nephelometric measurement of PM_{10} to ensure that the mass measured concentration remains independent of changes in the particle population being sampled (Thermo Fisher Scientific, 2007). The humidity levels are regulated by the intelligent moisture control system using a heating system that is linked to a

relative humidity sensor located upstream of the sample. This provides a representative measurement of the relative humidity at the particulate measurement (Thermo Fisher Scientific, 2007). The SHARP has a span drift of less than 0.02 % per day with an hourly precision of ± 2 μg/m³ for ambient concentrations lower than 80 μg/m³ and ± 5μg/m³ for values greater than 80 μg/m³ (Thermo Fisher Scientific, 2007).

3.4.7. BC

A multi-angle absorption photometer (MAAP), model 5012, analyser was used to measure atmospheric black carbon (BC) concentrations. The MAAP is based on the principle of aerosol-related light absorption and the corresponding atmospheric BC mass concentration (Thermo Fisher Scientific, 2007). The sample is drawn through the inlet and deposits onto a glass-fibre filter tape. The filter tape will accumulate an aerosol sample towards a threshold value, whereupon the filter tape will automatically advance prior to reaching saturation. A 670 nm visible light source is aimed at the deposited aerosol and filter tape matrix. Photo-detectors measure the transmitted and reflected light individually. The light beam is attenuated from an initial reference reading from a clean filter spot during the sample accumulation. Real-time data output is reached by continuous integration of the reduction of light transmission, multiple reflection intensities and air sample volume over the sample run period (Thermo Fisher Scientific, 2007). Additionally, all data was corrected based on the algorithm published relatively recently by Hyvärinen *et al.* (2013), which compensates for high atmospheric BC loading, which is commonly experienced at Welgegund when savannah and grassland fire plumes are sampled (Vakkari *et al.*, 2014; Hyvärinen *et al.*, 2013).

Chapter 4

Article

Chapter 4 consists of the article that was added into the dissertation in the exact format according to the journal's specifications.

A proxy for air quality over the Vredefort Dome world heritage area, South Africa

Running head: Air quality over the Vredefort Dome

Keywords: Vredefort Dome, World heritage site, Air quality, Welgegund, South Africa

Marcell Venter[1], Johan Paul Beukes*[1], Pieter Gideon van Zyl[1], Andrew Derick Venter[1], Kerneels Jaars[1], Miroslav Josipovic[1], Markku Kulmala[2], Ville Vakkari[3], Lauri Laakso[1,3]

1 Unit for Environmental Sciences and Management, North-West University, Potchefstroom, South Africa
2 Department of Physics, PO Box 64, FIN-00014, University of Helsinki, Finland
3 Finnish Meteorological Institute, Helsinki, Finland

Correspondence to: JP Beukes; e-mail: paul.beukes@nwu.ac.za; Postal address: Private Bag X6001, South Africa, Potchefstroom, 2520; Tel: +27 18 299 2337; Fax: +27 18 299 2350 (fax)

Abstract

The Vredefort Dome world heritage site in South Africa is the largest and second oldest meteorite impact structure in the world. Air quality in the Vredefort Dome can potentially be affected by the nearby declared air pollution priority areas and the Johannesburg-Pretoria megacity, which is well-known for high levels of atmospheric pollution. Notwithstanding the national and international importance of the Vredefort Dome, as well as the proximity of the afore-mentioned polluted source regions, currently, no air quality data is available for this area. In an effort to partially address the air quality knowledge gap, air masses passing over the Vredefort Dome were isolated and analysed at the Welgegund atmospheric measurement station as a proxy for ground-level air quality over the Vredefort Dome. The method had some limitations, since the frequency of such back trajectories was limited and those that did comply passed mostly over the cleaner south-western sector from the Vredefort Dome. Additionally, dilution during transport and aging of air masses after passing over the Vredefort Dome before arriving at Welgegund could also affect the pollutant levels observed. By comparing the results with South African air quality standards, it is evident that O_3 and PM_{10} exceeded the South African air quality standard limits. O_3 is a regional problem, while PM_{10} mostly originates from industries, household combustion and savannah/grassland fires. Although there were no exceedances recorded for SO_2 and NO_2 in air masses complying with the selection criteria, it is highly likely that such exceedances will occur over the Vredefort Dome.

Introduction

In 2007, it was announced that the Vredefort Dome will be proclaimed South Africa's seventh UNESCO (United Nations Educational, Scientific and Cultural Organization) world heritage site.[1,2] The Vredefort Dome is located on the boundary of the North West and the Free State Provinces of South Africa. The location thereof, within a regional context, is indicated in Figure 1a. It is the largest (diameter of 160 km) and the second oldest (~2 023 million years) meteorite impact structure in the world.[3] The Vredefort Dome is situated in the Witwatersrand basin of the Kaapvaal Craton.[4] The Witwatersrand basin contains ~40% of the world's gold resources, which was made accessible for exploitation by the uplifting of the mineral rich geological structures that took place as a result of the meteorite's impact.[5,6,7] The geological outcrops ('rings') of the Vredefort Dome can be observed in satellite images, as indicated in Figure 1c. As will be indicated in more detail later, the Vredefort Dome is also of particular significance from agricultural, tourism, historic, environmental, water supply and aesthetic perspectives.

Insert Figure 1

The Vredefort Dome is in relatively close proximity to several large atmospheric pollution source regions, i.e. the Vaal Triangle Airshed Priority Area (VTAPA), the Highveld Priority Area (HPA), the Waterberg Priority Area (WPA) and the Johannesburg-Pretoria (Jhb-Pta) megacity, as indicated in Figure 1b. The afore-mentioned three priority areas were declared by the South African government as air pollution hotspots, which indicates recognition by the national government that improvements in air quality within these regions are required.[8,9,10] The VTAPA mostly contains large petrochemical operations, pyro-metallurgical smelters and a coal-fired power station, with none of the afore-mentioned industrial sources removing sulphur dioxide (SO_2) and nitrogen oxides (NO_x) from their off-gas (de-SO_x and de-NO_x).[11,12] The large emission sources in the HPA include eleven coal-fired power stations (responsible for the majority of South Africa's electricity generation), several pyro-metallurgical smelters, char plants and a very large petrochemical operation, also without de-SO_x and de-NO_x technologies at all these sources.[12,13,14] An NO_2 hotspot, of which the tropospheric NO_2 column density is comparable to some of the most polluted areas in the world, is clearly visible over this area from satellite observations.[15] The WPA contains a large fraction of South Africa's mineral assets. In this area, 11 pyrometallurgical smelters occur within approximately 55 km radius, as well as two large coal-fired power stations.[16,17] The platinum

group metal (PGM) smelters in this area apply de-SO_x technology (e.g. Westcott18), but not de-NO_x, while none of the other smelters (e.g. ferrochrome and ferrovanadium) and the coal-fired power stations apply de-SO_x or de-NO_x technologies. Venter19 indicated that air quality of certain areas within the WPA is poor. Furthermore, the Vredefort Dome could also be affected by air masses passing over the Jhb-Pta conurbation, which is one of the 40 largest metropolitan areas in the world with a population of over 10 million.[15] Lourens15 indicated that the air quality in the Jhb-Pta megacity is in some aspects even worse than air quality in the HPA.

Because of the relatively close proximity of the perimeter of the VTAPA (~16 km), the HPA (~73 km), the WPA (~69 km) and the Jhb-Pta megacity (~64 km), it is likely that the air quality in the Vredefort Dome area will be influenced by these source regions. Additionally, the WPA lies upwind of the Vredefort Dome on the dominant anti-cyclonic recirculation path that traps and recirculates pollutants over the South African interior.[20,21] Notwithstanding the national and international importance of the Vredefort Dome, as well as the proximity thereof to major atmospheric pollution source regions in the South African interior, there are currently no air quality measurements being conducted within this proclaimed heritage area. The recently compiled management plan, as required by the UNESCO declaration, also highlighted this deficiency.[22] In an effort to partially address this knowledge gap, an air quality assessment, based on air masses that had passed over the Vredefort Dome before arriving at the Welgegund atmospheric measurement station, is presented in this paper as a proxy for ground-level air quality over the Vredefort Dome.

Site descriptions

The Vredefort Dome World Heritage Site is ~120 km south-west from Johannesburg. This heritage site includes the main area of the meteorite impact structure phenomenon that has a total surface area of 30 108 ha, as well as three geological (outcrop) satellite sites of 1 ha each.[1,2] The Vredefort Dome region is protected against external developments by a 5 km buffer zone surrounding the area.[1] It consists of 149 privately-owned properties that cover most of the surface area, with 600 ha being state owned. Land use on the private properties includes agriculture, game farming, resort accommodation, youth camps, team building and other tourism activities.[2] The Dome contains historical evidence of former human activities, such as stone age caves with tools and human remains, Khoi-San (Bushman) rock art, remnants of the Anglo-Boer War and old gold mines, all of which contribute to the South African cultural heritage.[2] The Vaal River, one of the longest rivers in South Africa and tributary of the Orange River, flows through the Vredefort Dome. It is the key water source for Johannesburg and east-central South Africa, and provides unique scenery and aesthetic

value within the Dome.[2] The Dome area is also rich in diverse indigenous plants, animals and bird species.[2]

Atmospheric measurements were conducted at the Welgegund monitoring station (black star in Figure 1a) (www.welgegund.org) (26°34'10"S, 26°56'21"E, 1480 m above mean sea level) situated ~100 km west of Johannesburg and ~25 km north-west from the city of Potchefstroom. Numerous previous papers have described the Welgegund measurement station, its surroundings and measurements conducted;[11,23-28] therefore, only a synopsis is presented. The station is located on a commercial farm and surrounded by grassland savannah. The Welgegund monitoring station is representative of a regional background site with no nearby significant anthropogenic pollution sources. Clean background air originates from the western sector (from north to south-east) that contains no major point sources.[11,23,27] However, pollution plumes can be observed form the priority areas and the Jhb-Pta megacity,[11,23,27] as well as from regional savannah and grassland fires that are common in the dry season in South Africa.[27-30] The Welgegund measurement station is ~66 km from the centre of the Vredefort Dome World Heritage area and is most-likely the closest comprehensively equipped atmospheric monitoring station.

Methods

Measurement methods

Measurements were conducted for a sampling period from 1 June 2010 to 28 February 2014. As presented in previous papers,[11,23,24,25,27,28] the Welgegund monitoring station holds a comprehensive set of continuous measurements. Of relevance to this paper were the measurements related to atmospheric SO_2, nitrogen oxide (NO), nitrogen dioxide (NO_2), ozone (O_3), carbon monoxide (CO) and particulate matter (PM) with an aerodynamic diameter ≤ 10 µm (PM_{10}). These species were measured with the following instruments: a Thermo-Electron 43S SO_2 analyser (Thermo Fisher Scientific Inc., Yokohama-shi, Japan), a Teledyne 200AU NO/NO_x analyser (Advanced Pollution Instrumentation Inc., San Diego, Cam USA), an Environment SA 41M O_3 analyser (Environment SA, Poissy, France), a Horiba APMA-360 CO analyser (Horiba, Kyoto, Japan), and a synchronised hybrid ambient real-time particulate (SHARP) monitor (model 5030, Thermo Fisher Scientific Inc.). Ancillary data utilised included atmospheric black carbon (BC) concentrations measured with a multi-angle absorption photometer (MAAP) (model 5012 Thermo Fisher Scientific Inc.), PM light scattering measured simultaneous at three wavelength (450, 525 and 635 nm) (Ecotech Aurora 3000) and meteorology measurements such as rain depth, temperature and relative humidity (RH), wind speed and direction, as well as fire occurrences (derived from satellite measurements). Rain intensity and depth was measured with a tip bucket rain intensity

meter (Vaisela QMR102); temperature and RH were measured with a Rotronic MP 101A instrument; and wind speed and direction were measured with the Vector A101ML and A200/L.

The Welgegund monitoring station was visited at least once a week for maintenance and for other *ad hoc* procedures. For quality assurance, the data was downloaded and visually inspected daily. If irregularities were observed in the data or in the instrumental diagnostic signals, the site was visited on the same day to rectify the problem. An electronic diary, recording all site visits and actions taken, was also kept. As previously described,[14,16,19,24,31,32] the raw high resolution atmospheric data collected at Welgegund was visualised and corrected with a fit-for-purpose MATLAB program set. Firstly, periods of poor or uncertain data quality, e.g. during power failures and recovery thereafter or during site visits when work was conducted that could have influenced the data, were rejected. The data was then automatically corrected based on calibrations (zero and span), as well as flow checks. The measured 1-min high resolution data was converted to 15 min averages after the afore-mentioned quality assurance procedures were applied. A 15 min average was only calculated if at least two thirds of the 1-min data were available. The conversion of measured gaseous mixing ratio (in parts per billion by volume, ppbv) to µg/m³ was conducted at standard temperature and pressure (0 °C and 101.3 kPa).

The identification of savannah and grassland fire burn scar pixels was based on remote-sensing observations from the Moderate Resolution Imaging Spectroradiometer (MODIS) collection 5 burned area product.[33]

Analysis of air mass histories and association with in situ measurements

HYSPLIT 4.8 (HYbrid Single-Particle Lagrangian Integrated Trajectory) was used to calculate 96-hour back trajectories, arriving hourly at the Welgegund measurement station, for the entire measurement period with an arrival height of 100 m.[34] An arrival height of 100 m was chosen because the orography in HYSPLIT is not very well defined, and therefore lower arrival heights could result in increased error margins on individual trajectory calculations. Considering the above, 24 hourly-arriving back trajectories for each day were calculated for the entire sampling period.

In order to obtain a statistical overview of air mass history, overlay back trajectory maps were generated. This was conducted by superimposing individual back trajectories generated in HYSPLIT with a fit-for-purpose MATLAB script on maps that were divided into 0.2 X 0.2°grid cells. Colour was used to indicate the normalised percentage of trajectories

passing over specific grid cells, with red and dark blue representing the highest and lowest percentages, respectively.

In addition to the above-mentioned overlay back trajectory maps, individual back trajectories were also sorted in order to identify back trajectories that had passed over the Vredefort Dome area before arriving at Welgegund, but did not pass over significant sources after passing over the Dome. This was accomplished by firstly defining polygons representing the surface areas of the proclaimed Vredefort Dome area, the city of Potchefstroom that lies between the Vredefort Dome and Welgegund, as well as an area that included the Jhb-Pta megacity and all the large point sources (e.g. coal-fired power stations, metallurgical smelters and large petrochemical operations) occurring within the previously mentioned declared airshed priority areas. The latter area is subsequently referred to as the Large Point Source (LPS) region. Figure 2a indicates an example of trajectory considered to be appropriate, while Figure 2b and 2c indicate examples of trajectories that had passed over the Vredefort Dome that subsequently pass over either the LPS region or over Potchefstroom, respectively, before arriving at Welgegund.

Insert Figure 2

The 15 min average data of the *in situ* pollutant species measured at Welgegund was linked to the air mass history by associating every selected hourly-arriving back trajectory, with the two 15 min averages before the hourly arrival time, as well as the two 15 min averages after the hourly back trajectory arrival time. This implies that each selected back trajectory was associated with four 15 min averages of the *in situ* measurements.

Results

General meteorological characterisation and savannah/grassland fire frequencies

In Figures 3a to 3c, variations in monthly precipitation, temperature and relative humidity (RH), as measured at Welgegund for the entire monitoring period (1 June 2010 – 28 February 2014), are presented. A wind rose, indicating wind direction and speed, also for the entire monitoring period at Welgegund, is indicated in Figure 3d. Although these meteorological parameters were measured at Welgegund and not in the Vredefort Dome area, the proximity of Welgegund to the Dome makes these parameters relevant, at least

within a general atmospheric perspective, in order to explain possible seasonal influences on the Vredefort Dome's air quality. Additionally, Figure 3e presents the monthly variations in fire burn scar pixel counts within a 500 km radius, as measured from the centre of the Vredefort Dome area.

Insert Figure 3

Air mass history

Figure 4a indicates a normalised overlay back trajectory map for air masses arriving at the centre of the Vredefort Dome during the entire monitoring period, without any selection criteria applied. The LPS region is also shown on this map in order to indicate its possible influence on air quality in the Dome area. From this figure, it is evident that air quality in the Vredefort Dome will be influenced by air masses that have circulated in an anti-cyclonic manner around the LPS region or air masses that had passed over the LPS region, where it has been shown that air quality is problematic.

The overlay back trajectory map for air masses that had passed over the Vredefort Dome before arriving at the Welgegund measuring site (black star), according to the selection criteria (Section 3.2 and Figure 2), for the entire sampling period, is presented in Figure 4b. Figure 4b indicates that most of the general air flow of the selected air masses was from the relatively cleaner south-western sector from the Vredefort Dome, while in reality the Vredefort Dome's air quality is more influenced by the LPS region and by air masses that are recirculated around this source region, as indicated by Figure 4a, where no selection criteria were applied.

Insert Figure 4

The numbers (N) of trajectories that complied with the selection criteria (Section 3.2 and Figure 2) per month and the percentage that it represented of all the hourly-arriving back trajectories calculated for a specific month, are indicated in Figure 5. As is evident from these results, the percentages of trajectories that complied with the selection criteria were relatively low and varied between 0.4 and 13.5% of all calculated trajectories per month. There was no seasonal pattern in Figure 5, which is good, since it implies that the back

trajectory selection criteria will not bias the associated *in situ* measurement data that was used to determine proxies for air quality in the Vredefort Dome.

Insert Figure 5

In order to further differentiate between air masses that had passed over the LPS region and those that did not, two additional normalised overlay trajectory maps were generated. This was achieved by considering the back trajectories that complied with the initial selection criteria (Section 3.2 and Figure 2) as indicated in Figure 4b and additionally dividing these selected back trajectories into two groups, i.e. those that had passed over the LPS region (Figure 4c) and those that had not passed over the LPS region (Figure 4d).

All the normalised overlay back trajectory maps (Figure 4a to 4d), together with the previously presented measured meteorological data and fire pixel counts (Figures 3a to 3e), will be considered in subsequent discussions to contextualise the air quality data.

Air quality assessment

The South African National Ambient Air Quality Standards (NAAQS), with associated limits, are presented in the first four columns of Table 1. From these standards, it is evident that certain averaging periods should be calculated for certain pollutant species in order to assess whether pollutant concentrations exceed standard limits. For legislation relating to a 10-min averaging period, i.e. for SO_2, each of the four 15-min average SO_2 values measured at Welgegund that was associated with the selected back trajectory arrival time could be compared to the legislative requirement. Similarly, for the one-hour legislatively averaging periods, i.e. for SO_2, NO_2 and CO, the selected back trajectory arrival times could be correlated directly with the average of the four 15-min values associated with the back trajectory arrival time. However, for the longer legislative averaging periods, e.g. eight and 24 hours, it was not that straightforward, since the frequency of back trajectories that complied with the first selection criteria (Section 3.2 and Figure 2) was not very high (Figure 5) and therefore the probability of identifying eight or more consecutive hourly-arriving back trajectories that complied was low. In order to at least estimate possible exceedances of these longer legislative averaging periods, the 15-min average data that was correlated to the arrival times of the selected back trajectories was linearly interpolated and the averages were calculated from the interpolated data. Figures 6a to 6e represent the 15-min average *in situ* SO_2, NO_2, O_3, CO and PM_{10} data associated with the selected back

trajectory arrival times, as well as the linearly interpolated data for the entire sampling period. The NAAQS limits for the afore-mentioned atmospheric species, as presented in Table 1, are also indicated on these figures in order to facilitate further discussion with respect to air quality. The frequency of exceedances derived from this data is also presented Table 1.

Insert Table 1

Insert Figure 6

According to the proxies determined for concentrations of SO_2 and NO_2 in the Vredefort Dome, Table 1 and Figures 6a and b indicate that there were no exceedances observed for SO_2 and NO_2 for any of the averaging periods of the NAAQS. This absence of exceedances for these species can at least partially be attributed to the limitations of the method applied in this study, i.e. isolating back trajectories according to the selection criteria. Figure 4a clearly indicates that the LPS region has an effect on the Vredefort Dome, and it is well known that the LPS region has relatively high SO_2 and NO_2 ambient concentrations.[12,13,15,19] In addition to the afore-mentioned the median, 25th and 75th percentile times it takes for air masses to arrive at Welgegund after passing over the Vredefort Dome were calculated as 9, 5 and 16 hours, respectively. This indicates that SO_2 and NO_2 will further dilute, since no air mass overpass over additional point or area sources were allowed according to the selection criteria (Section 3.2 and Figure 2). During the afore-mentioned additional travelling time, SO_2 and NO_2 will also further oxidise to sulphate and nitrate.[13,27] The mean concentrations, calculated from *in situ* data associated with air masses complying with the selection criteria and gap filling with linear interpolation, for SO_2 and NO_2, were determined to be 3 and 5 ppb, respectively (Table 1). In Figure 7, a comparison of these means, with mean values reported for other continental sites in South Africa, is presented. From these comparisons it is evident that SO_2 concentrations in air masses that had passed over the Vredefort Dome exceeded the SO_2 concentrations reported for two background sites, i.e. Botsalano and Louis Trichardt with a factor of ~4.6 and ~4.1 respectively.[31,35] However, SO_2 concentrations were lower than SO_2 levels reported for sites within the LPS region.[12,14,19] The mean NO_2 concentration in the selected air masses passing over the Vredefort Dome also exceeded levels thereof at the two cited background sites (Botsalano and Louis Trichardt) with a factor of ~3.4 and ~6.4, respectively, and was comparable to several sites within the LPS region.

Insert Figure 7

The NAAQS for O_3 only has an eight-hour moving averaging limit that allows 11 exceedances per year. According to Table 1 and Figure 6c, the eight-hour moving average was exceeded 141 times per year. As indicated earlier the air masses isolated according to the selection criteria spend additional travelling time before being analysed at Welgegund, which could result in additional photochemical formation of O_3. However, O_3 is a regional southern African problem.[19,31,36-39] Therefore it is likely that O_3 will exceed the NAAQS limit as indicated by the air quality proxy determined here. The mean concentration for O_3 for the entire measurement period, also calculated from the linear interpolated data, was 30 ppb (Table 1). It is evident from the comparison presented in Figure 7 that the proxy for mean O_3 concentrations over the Vredefort Dome calculated in this study was comparable to O_3 mean values for sites within the LPS region and the two cited background sites. Tropospheric O_3 concentrations over South Africa have been increasing, most probably due to increasing Southern Hemisphere pollution.[38] In addition, daytime radiation from sunlight required for O_3 formation is not likely to be a limiting factor in sunny South Africa, while concentrations of O_3 precursor species (NO_2, volatile organic compound (VOCs) and CO) are relatively high in many regions in South Africa.[11,12,19,28] As previously mentioned, almost no industries in South Africa de-NO_x and, in addition, the vehicle fleet is relatively aged, leading to high NO_2 concentrations in the HPA and the Jhb-Pta megacity.[12,15] In contrast to, for instance, the boreal forest region and the Amazon, aromatic hydrocarbon VOC concentrations are in general higher than biogenic VOC concentrations in South Africa.[11,40] Furthermore, ambient CO concentrations, even in background areas, are elevated due to large-scale savannah and grassland fires in southern Africa.[28,41] Normalised O_3 concentrations, for air masses that complied with the first selection criteria (Section 3.2 and Figure 2) as indicated in Figure 4b, and additionally also had passed over the LPS region (Figure 4c) or not over the LPS (Figure 4d) are presented in Figure 8. From these results it is evident that the O_3 in air masses that had passed over the LPS region was marginally higher than the concentrations in air masses that had passed over the background region, but not significantly so. This confirms the earlier statement that O_3 is a regional southern African problem and that the Vredefort Dome area will most certainly be affected by O_3 pollution. One of the most probable impacts is related to O_3-induced vegetation damage. The recommended approach to assess this risk is based on stomatal O_3 flux data and the corresponding determination of the dose-response relationships of different plant species.[37,42,43] However, no such data exist

for South Africa. A less accurate, but widely used method is based on the application of AOT40, which is defined as the accumulated O_3 exposure above a threshold of 40 ppb during daylight hours of the growing season.[42] Although AOT40 is a European derived risk indicator, it has been applied in southern Africa.[37,44,45] Over the approximately four years of data considered in this study, the AOT40 calculated from *in situ* O_3 data associated with air masses complying with the selection criteria and gap filling with linear interpolation varied between 990 to 5781 ppb h/a during the growing season (October – February) and daylight hours (06:00 – 18:00 local time). This indicates that AOT40 can vary significantly from year-to-year and that considerable exceedances of the 3000 and 5000 ppb h/a European guidelines for crop and tree damage, respectively, can occur.[37,42,43]

Insert Figure 8

No exceedances were observed for CO (Table 1 and Figure 6d) for any of the averaging periods. Comparing the mean CO concentration, calculated from *in situ* data associated with air masses complying with the selection criteria and gap filling with linear interpolation, i.e. 148 ppb, with the CO mean concentrations reported for a background site at Botsalano (104 ppb)[31] and a site in the WPA (230 ppb),[19] it is evident that the CO concentration in the Vredefort Dome is approximately 1.4 times higher than the background site, but is approximately 1.6 times lower than the site in the LPS region (which was located in the WPA).

Considering PM_{10}, Table 1 and Figure 6e indicate that there were 17 exceedances of the 24-hour NAAQS average limit and no exceedances for the annual NAAQS average limit per year. It can be assumed that even more PM_{10} exceedances occurred over the Vredefort Dome than what the calculated proxies indicate due to two reasons. Firstly, the data gap observed in Figure 6e was not gap filled (linear interpolation) and therefore no exceedances were reported in this time period. The gap was due to PM_1, instead of PM_{10}, measurements conducted between September 2010 and August 2011 at Welgegund in order to correlate PM_1 mass with PM_1 aerosol chemical composition.[27] Secondly, the additional travelling time of air masses passing over the Vredefort Dome before being analysed at Welgegund will result in additional atmospheric removal of PM_{10}.

Data from the three-wavelength nephelometer was used to confirm that the PM_{10} exceedances reported were not as a result of localised dust emissions, but really due to

more distant sources. Additionally, as will be indicated later, the seasonal pattern observed for PM_{10} in air masses that complied with the selection criteria was very similar to those of CO and BC. This indicates that the PM_{10} exceedances were mostly due to combustion sources, e.g. industrial fossil fuel use, household combustion, and savannah and grassland fire.

The PM_{10} mean concentration obtained from the interpolated data (Table 1 and Figure 6d) was 28 µg/m^3, which was lower with a factor of ~1.5 than the mean concentration observed at a site in the WPA in the LPS region,[19] but higher with a factor of ~1.5 than the background site at Botsalano.[31] A comparison of the normalised mean concentration for air masses that had passed over the background region (Figure 4d) with air masses that had passed over the LPS region (Figure 4c) in Figure 8 indicates no substantial differences between the mean concentrations. However, more LPS overpass trajectories have significantly larger PM_{10} concentrations, as indicated by the larger spread in normalised concentrations. This indicates that the Vredefort Dome is on occasion impacted by air masses that had passed over the LPS regions that have very high PM_{10} concentrations.

The monthly concentrations of SO_2, NO_2, O_3, CO, PM_{10} and black carbon (BC) for the entire sampling period, in air masses selected according to the selection criteria (Section 3.2 and Figure 2) were also considered. No distinct seasonal patterns were observed for SO_2 and NO_2. The lack in seasonality can in all likelihood be attributed to the relatively low frequencies of air masses that were identified according to the selection criteria, as was indicated in Figure 5. Additionally, SO_2 and NO_2 in the South African interior mostly originate form continuous operating industrial sources, e.g. metallurgical smelters,[19] as well as from coal-fired power stations and petrochemical operations.[12,13] As is indicated in Figure 9, O_3, CO, PM_{10} and BC indicated more distinct seasonal patterns in air masses selected according to the selection criteria (Section 3.2 and Figure 2). The highest levels of O_3 concentrations occurred during the late spring and early summer months (Figure 9a), which corresponds with observations by Venter19 and Laakso31. CO and BC mostly peaked during the drier (Figure 3a and 3c) months, with higher fire frequencies (Figure 3e), as well as during the colder months (Figure 3b), when household combustion for space heating is prevalent.[19] PM_{10} also peaked during similar periods than CO and BC, indicating similar sources.

Insert Figure 9

Conclusions

As far as the authors could assess, this is the first air quality assessment of the Vredefort Dome world heritage site published in the peer-reviewed public domain. The air quality was assessed by identifying back trajectories that had passed over the Vredefort Dome and that had not passed over significant source areas thereafter, before arriving at the Welgegund atmospheric monitoring station. The method had some limitations, since the frequency of such back trajectories was limited, while those that did comply passed mostly over the cleaner south-western sector of the Vredefort Dome. Additionally, dilution during transport and aging of air masses after passing over the Vredefort Dome before arriving at Welgegund could also affect the pollutant levels observed. Overlay back trajectory maps indicated that the Vredefort Dome was impacted much more by more polluted areas in the LPS region compared to the back trajectories adhering to the criteria applied that were used in the air quality assessment of the Vredefort Dome. Therefore, the air quality proxies presented in this study can be considered as an underestimation of pollutant levels. By comparing the results obtained in this study with the NAAQS, it is evident that O_3 and PM_{10} exceeded the NAAQS limits. O_3 is a regional problem, while PM_{10} mostly originates from industries, household combustion and savannah/grassland fires. Even though there were no exceedances recorded for SO_2 and NO_2 in air masses complying with the selection criteria, it is highly likely that such exceedances will occur over the Vredefort Dome. However, the afore-mentioned limitation in the method prevented observations thereof.

References

1. World Heritage convention act, 1999 (No. 49 of 1999) Proclamation of Vredefort Dome as world heritage site. Government Gazette. No. 30590 [online]. 2007 [cited 2015 May 27]. Available from: http://www.gov.za/documents/world-heritage-convention-act-proclamation-vredefort-dome-world-heritage-site-comments

2. UNESCO (United Nations Educational, Scientific and Cultural Organization). Vredefort Dome -Nomination [online]. 2005 [2015; cited 2015 May 27]. Available from: http://whc.unesco.org/en/list/1162/documents/

3. GSIS outstanding website. Earth Impact Database [online]. Fredericton: Spray, J.; 2011 [2015; cited 2015 May 25]. Available from: http://www.passc.net/EarthImpactDatabase/

4. Harris, C., Fourie, D.S., Fagereng, A. Stable isotope for impact-related pseudotachylite formation at Vredefort by local melting of dry rocks. S. Afr.J.Geol. 2013;116.1:101-118. doi:10.2113/gssajg.ll6.1.101.

5. Gibson, R.L., Reimold, W.U. The significance of the Vredefort Dome for the thermal and structural evolution of the Witwatersrand Basin, South Africa. Miner. Petrol. 1999;66:5-23. http://dx.doi.org/10.1007/BF01161720.

6. Minter, W.E.L., Goedhart, M., Knight, J., Frimmel, H.E. Morphology of Witwatersrand gold grains from the Basal Reef: evidence for their detrital origin. Econ. Geol. 1993;88(2):273-248. doi: 10.2113/gsecongeo.88.2.237.

7. Parys.co.za. The Vredefort Dome: Centre of the world's largest meteorite impact structure [online]. Reimold, W.U.; [2015; cited 2015 May 25]. Available from: http://www.parys.co.za/parys/vredefort-dome.html

8. Declaration of the Vaal Triangle air-shed priority area in terms of section 18(1) of the National Environmental Management: Air Quality Act 2004, (Act no. 39 of 2004). Government Gazette. No. 28732 [online]. 2006 [cited 2015 June 3]. Available from: https://www.environment.gov.za/legislation/gazetted_notices/archived_gazetted_notices

9. Declaration of the Highveld aspriority area in terms of Section 18(1) of The National Environmental Management: Air Quality Act, 2004 (Act no. 39 of 2004). Government Gazette. No. 30518 [online]. 2007 [cited 2015 June 3]. Available from:

https://www.environment.gov.za/legislation/gazetted_notices/archived_gazetted_notices

10. National Environmental Management: Air Quality Act, 2004 (Act no. 39 of 2004): declaration of the Waterberg National prioriy area. Government Gazette. No. 33600 [online]. 2012 [cited 2015 June 3]. Available from: https://www.environment.gov.za/legislation/gazetted_notices

11. Jaars, K., Beukes, J.P., Van Zyl, P.G., Venter, A.D., Josipovic, M., Pienaar, J.J., et al. Ambient aromatic hydrocarbon measurements at Welgegund, South Africa. Atmos. Chem. Phys. 2014;14:7075-7089. doi:10.5194/acp-14-7075-2014.

12. Lourens, A.S., Beukes, J.P., Van Zyl, P.G., Fourie, G.D., Burger, J.W., Pienaar, J.J., et al. Spacial and temporal assessment of gaseous pollutants in the Highveld of South Africa. S. Afr. J. Sci. 2011;107(1):1-8. doi: 10.4102/sajs.v107i1/2.269.

13. Collett, K.S., Piketh, S.J., Ross, K.E. An assessment of the atmospheric nitrogen budget on the South African Highveld. S. Afr. J. Sci. 2010;106(5):1-9. doi: 10.4102/sajs.v106i5/6.220.

14. Laakso, L., Vakkari, V., Laakso, H., Virkkula, A., Kulmala, M., Beukes, J.P., et al. South African EUCAARI measurements: seasonal variation of trace gases and aerosol optical properties. Atmos. Chem. Phys. 2012;12:1847–1864. doi:10.5194/acp-12-1847-2012.

15. Lourens, A.S.M., Butler, T.M., Beukes, J.P., Van Zyl, P.G., Beirle, S., Wagner, T.K., et al. Re-evaluating the NO_2 hotspot over the South African Highveld. S. Afr. J. Sci. 2012;108(11):1-6. doi.org/10.4102/sajs.

16. Hirsikko, A., Vakkari, V., Tiitta, P., Manninen, H.E., Gagne, S., Laakso, H., et al. Characterisation of sub-micron particle number concentrations and formation events in the western Bushveld Igneous Complex, South Africa. Atmos. Chem. Phys. 2012;12:3951-3967. doi:10.5194/acp-12-3951-2012.

17. Van Zyl, P.G., Beukes, J.P., Du Toit, G., Mabaso, D., Hendriks, J., Vakkari, V., et al. Assessment of atmospheric trace metals in the western Bushveld Igneous Complex, South Africa. S. Afr. J. Sci. 2014;110:1-11. http://dx.doi.org/10.1590/sajs.2014/20130280.

18. Westcott, G., Tacke, M., Schoeman, N., Morgan, N. Impala Platinum smelter, Rustenburg – an integrated smelter off-gas treatment solution. J. S. Afr. I. of Min. Metall. 2007;107:281-287.

19. Venter, A.D., Vakkari, V., Beukes, J.P., Van Zyl, P.G., Laakso, H., Mabaso, D., et al. An air quality assessment in the industrialized western Bushveld Igneous Complex, South Africa. S. Afr. J. Sci. 2012;108(9):1-10. http:// dx.doi.org/10.4102/sajs. v108i9/10.1059.

20. Garstang, M., Tyson, P.D., Swap, R., Edwards, M., Kållberg, P., Lindesay, J.A. Horizontal and vertical transport of air over southern Africa. J. Geophys. Res. 1996;101(D19):721-736. *doi:10.1029/95JD00844.*

21. Tyson, P.D., Garstang, M., Swap, R. Large-scale re-circulation of air over southern Africa. J.Appl. Meteorol. 1996;35:2218-2236. http://dx.doi.org/10.1175/1520-0450(1996)035<2218:LSROAO>2.0.CO;2.

22. Environmental Affairs. Environmental Management Framework for Vredefort Dome World Heritage Site (VDWHS) and Moqhaka and Ngwathe Local Municipalities in the Free State Province [online]. The Centre for Environmental Management (CEM); 2013 [2015;cited 2015 May 27] Available from: https://www.environment.gov.za/environmental_management_frameworkvredefort_domeworld_heritagesite

23. Beukes, J.P., Vakkari, V., Van Zyl, P.G., Venter, A.D., Josipovic, M., Jaars, K., et al. Source region plume characterisation of the interior of South Africa as observed at Welgegund. Clean Air J. 2013;23(1):7-10.

24. Beukes, J.P., Venter, A.D., Josipovic, M., Van Zyl, P.G., Vakkari, V., Jaars, K., et al. Automated continuous air monitoring. In: Forbes, P.B.C, editor. Monitoring of air pollutants – sampling, sample, preparation and analytical techniques. ed. [1st]. Amsterdan: Elsevier; 2015. p. 183–208.

25. Booyens, W., Van Zyl, P.G., Beukes, J.P., Ruiz-Jimenez, J., Kopperi, M., Riekkola, M., et al. Size-resolved characterisation of organic compounds in atmospheric aerosols collected at Welgegund, South Africa. J. Atmos. Chem. 2015;72:46-64. doi 10.1007/s10874-015-9304-6.

26. Kuik, F., Lauer, A., Beukes, J.P., Van Zyl, P.G., Josipovic, M., Vakkari, V., et al. The anthropogenic contribution to atmospheric black carbon concentrations in southern

Africa: a WRF-Chem modeling study. Atmos. Chem. Phys. 2015;15:7309-7363. doi:10.5194/acpd-15-7309-2015.

27. Tiitta, P., Vakkari, V., Josipovic, M., Croteau, P., Beukes, J.P., Van Zyl, P.G., et al. Chemical composition, main sources and temporal variability of PM_1 aerosols in southern African grassland. Atmos. Chem. Phys. 2014;13:15517-15566. doi:10.5194/acp-14-1909-2014.

28. Vakkari, V., Kerminen, V.-M., Beukes, J.P., Tiitta, P., Van Zyl, P.G., Josipovic, M., et al. Rapid changes in biomass burning aerosols by atmospheric oxidation. Geophys. Res. Lett. 2014;41:2644-2651. doi:10.1002/2014GL059396.

29. Hyvärinen, A.-P., Vakkari, V., Laakso, L., Hooda, R.K., Sharma, V.P., Panwar, T.S., et al. Correction for a measurement artifact of the Multi-Angle Absorption Photometer (MAAP) at high black carbon mass concentration levels. Atmos. Meas. Tech. 2013;6:81-90. doi:10.5194/amt-6-81-2013.

30. Jayaratne, E.R., Verma, T.S. The impact of biomass burning on the environmental aerosol concentration in Gaborone, Botswana. Atmos. Environ. 2001;35:1821-1828. doi:10.1016/S1352-2310(00)00561-6.

31. Laakso, L., Laakso, H., Aalto, P.P., Keronen, P., Petäjä, T., Nieminen, T., et al. Basic characteristics of atmospheric particles, trace gases and meteorology in a relatively clean Southern African Savannah environment. Atmos. Chem. Phys. 2008;8:4823-4839.

32. Vakkari, V., Laakso, H., Kulmala, M., Laaksonen, A., Molefe, M., Kgabi, N., et al. New particle formation events in semi-clean South African savannah. Atmos. Chem. Phys. 2011;11:3333-3346. doi:10.5194/acp-11-3333-2011.

33. Roy, D.P., Boschetti, L., Justice C.O., Ju, J. The collection 5 MODIS burned area product – Global evaluation by comparison with the MODIS active fire product. Remote Sens. Environ. 2008;112(9):3690-3707. doi:10.1016/j.rse.2008.05.013.

34. Air Resources Laboratory, National Oceanic and Atmospheric Administration (NOAA). HYSPLIT Model [online]. [2015; 2014 Feb11]. Available from: http://www.arl.noaa.gov

35. Martins, J.J. Concentrations and deposition of atmospheric species at regional sites in southern Africa [MSc thesis]. Potchefstroom: North-West University; 2009.

36. Josipovic, M., Annegarn, H.J., Kneen, M.A., Pienaar, J.J, Piketh, S.J. Concentrations, distributions and critical level exceedance assessment of SO_2, NO_2 and O_3 in South Africa. Environ. Monit. and Assess. 2010;171:181-196. doi 10.1007/s10661-009-1270-5.

37. Laakso, L., Beukes. J.P., Van Zyl, P.G., Pienaar, J.J., Josipovic, M., Venter, A.D., et al. Ozone concentrations and their potential impacts on vegetation in Southern Africa. In: Matyssek, R., Clarke, N., Cudlin, P., Mikkelsen, T. N., Tuovenin, J.-P., Wieser, G., Paoletti, E., editors. Developments in Environmental Science. ed. [1st]. Kidlington: Elsevier; 2013. p. 429–450.

38. Thompson, A.M., Balashov, N.V., Witte, J.C., Coetzee, J.G.R., Thouret, V., Posny, F. Tropospheric ozone increases over the southern Africa region: bellwether for rapid growth in Southern Hemisphere pollution? Atmos. Chem. and Phys. 2014;14:9855-9869. doi:10.5194/acp-14-9855-2014.

39. Zunckel, M., Koosailee, G., Yarwood, G., Maure, G., Venjonoka, K., Van Tienhoven, A.M., et al. Modelled surface ozone over southern Africa during the Cross Border Air Pollution Impact Assessment Project. Environ. Modell. Softw. 2006;21:911-924. doi:10.1016/j.envsoft.2005.04.004.

40. Otter, L.B., Geunther, A., Greenberg, J. Seasonal and spatial variations in biogenic hydrocarbon emissions form southern African savannas and woodlands. Atmos. Environ. 2002;36:4265-4275. doi:10.1016/S1352-2310(02)00333-3.

41. Annegarn, H.J., Otter, L.B., Swap, R.J., Scholes, R.J. Southern Africa's ecosystem in a test-tube: a perspective on the Southern African Regional Science Initiative (SAFARI 2000): commentary. S. Afr. J. Sci. 2002;98:111-113.

42. CLRTAP. Mapping Critical Levels for Vegetation, Chapter III of Manual on methodologies and criteria for modelling and mapping critical loads and levels and air pollution effects, risks and trends. UNECE Convention on Long-range Transboundary Air Pollution. Geneva: 2015 [2013 May 28; 2015 Nov 18]. Available from: www.icpmapping.org

43. Grünhage, L., Matyssek, R., Wieser, G., Häberle, K.-H., Leuchner, M., Menzel, A., et al. Flux-based ozone risk assessment for adult beech and spruce forests. Dev. Environ. Sci. 2013;13:251–266. doi 10.1007/s00468-012-0716-5.

44. Avnery, S., Mauzerall, D.L., Liu, J., Horowitz, Larry W. Global crop yield reductions due to surface ozone exposure: 1. Year 2000 crop production losses and economic damage. Atmos. Environ. 2011;45:2284–2296. doi:10.1016/j.atmosenv.2010.11.045.

45. Van Tienhoven, A., Zunckel, M., Emberson, L., Koosailee, A., Otter, L. Preliminary assessment of risk of ozone impacts to maize (zea mays) in southern Africa. Environ. Pollut. 2006;140:220–230. doi:10.1016/j.envpol.2005.07.016.

Figure 1: (a) The location of the Vredefort Dome within a regional context. (Countries: Nam – Namibia, Bot – Botswana, Zim – Zimbabwe, Moz – Mozambique, Sz – Swaziland, Les – Lesotho, South African provinces: WC – Western Cape, EC – Eastern Cape, NC – Northern Cape, FS – Free State, KZN – KwaZulu-Natal, NW – North West, MP – Mpumalanga, LP – Limpopo Province) (b) The positioning of the Welgegund monitoring station and spatial extent of the declared priority areas and the Jhb-Pta megacity, as well as very large point sources in the South African interior are indicated on the zoomed-in map. (c) A Google Earth image of the area clearly indicating the rings that form part of the Vredefort Dome impact structure.

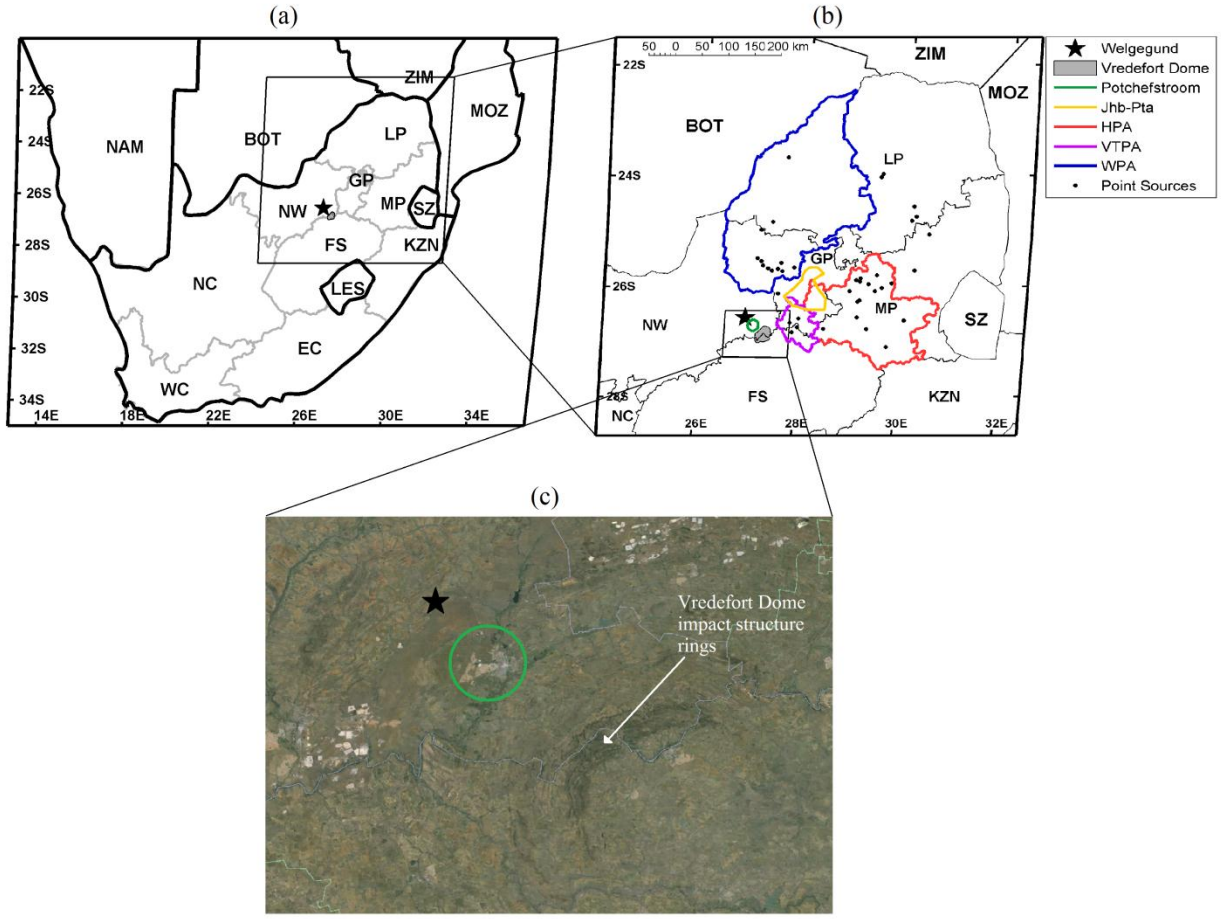

Figure 2: (a) An example of a back trajectory that had passed over the Vredefort Dome before arriving at Welgegund, but that did not pass over either Potchefstroom or the LPS region after passing over the Dome. (b) and (c) are examples of the back trajectories that had passed over the Vredefort Dome, but that did not comply with the selection criteria indicated in (a).

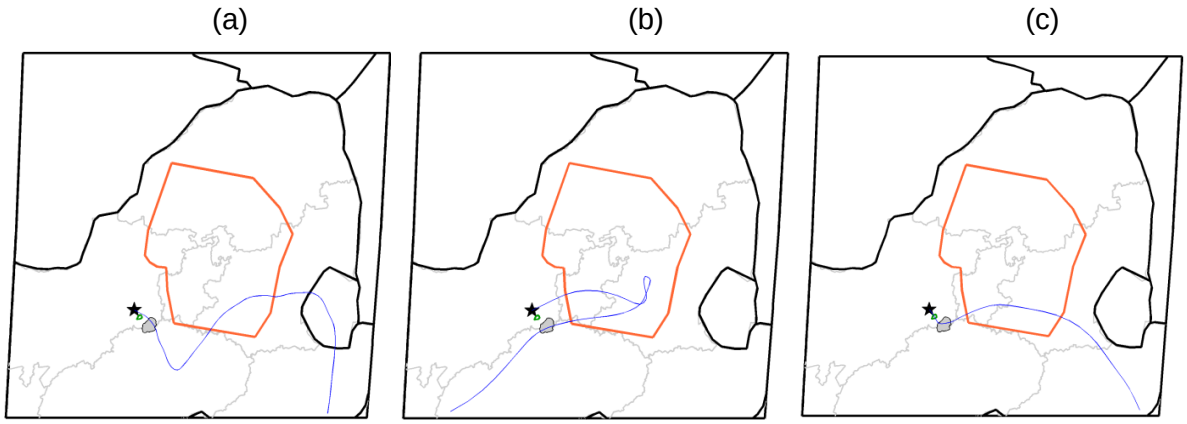

Figure 3: (a) Cumulative monthly precipitation, (b) temperature, (c) relative humidity, and (d) wind speed and direction measured at Welgegund for entire the sampling period. (e) Monthly variations in fire burn scar pixel counts within a 500 km radius, as measured from the centre of the Dome area. In (a), (b), (c) and (e), the dots indicate the median and the whiskers the 25th and 75th percentiles.

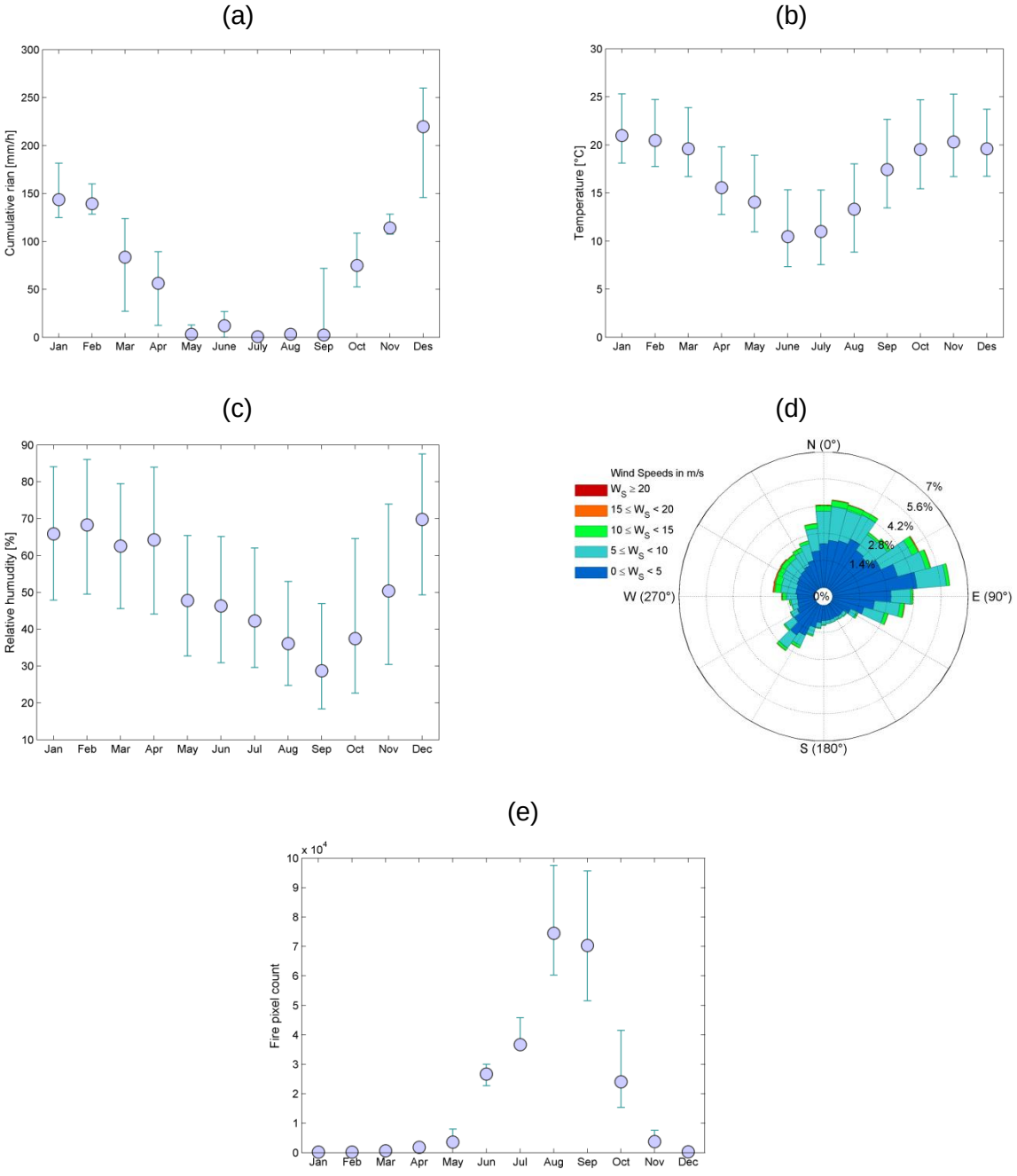

Figure 4: Overlay back trajectory map of (a) all back trajectories arriving at the centre of the Vredefort Dome for the entire monitoring period, (b) only back trajectories that complied with the selection criteria arriving at Welgegund, (c) only back trajectories that complied with the selection criteria arriving at Welgegund, which had also passed over the the LPS region, and (d) only back trajectories that complied with the selection criteria arriving at Welgegund, which did not pass over the LPS region.

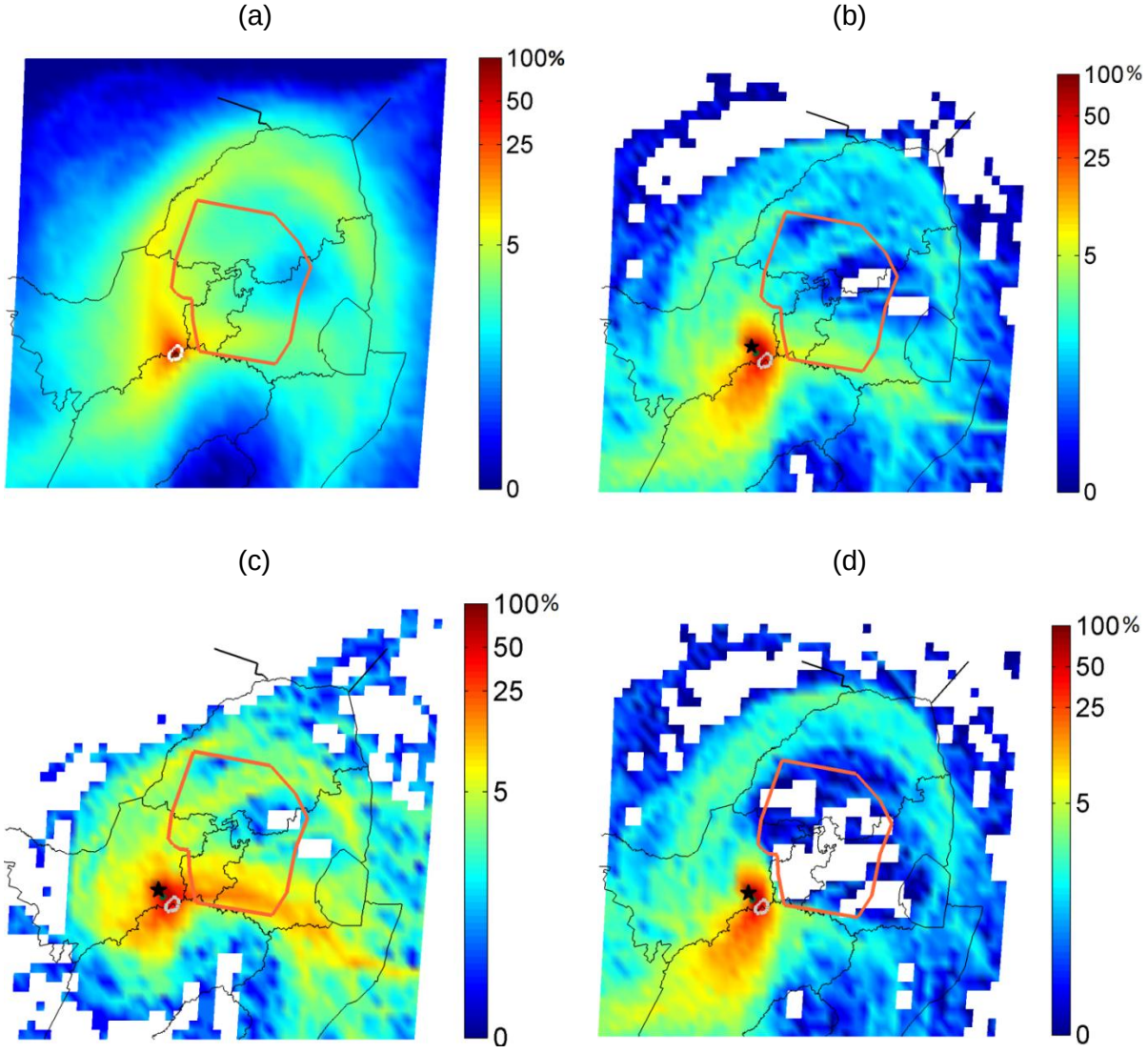

Figure 5: The total number (N) of trajectories per month that complied with the selection criteria for the entire sampling period. The percentages above each bar indicate the afore-mentioned N as a percentage of all the back trajectories calculated per month.

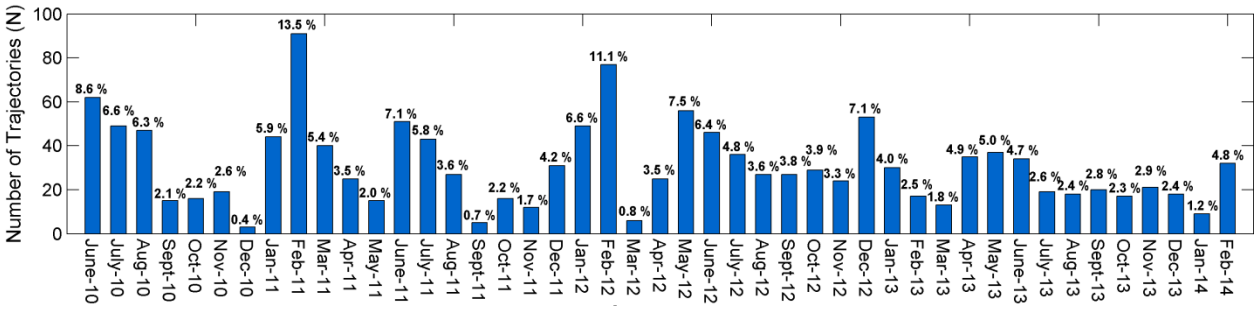

Figure 6: The 15-min average *in situ* pollutant concentration data that was correlated with the arrival times of the selected back trajectories and linear interpolation of this data for (a) SO_2, (b) NO_2, (c) O_3, (d) CO and (e) PM_{10} for the entire sampling period. The NAAQS limits for the afore-mentioned atmospheric species are also indicated.

(a)

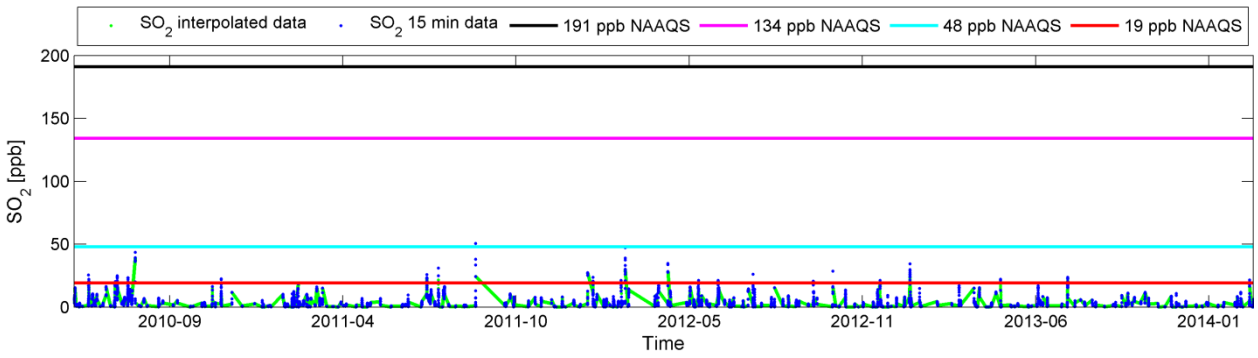

(b)

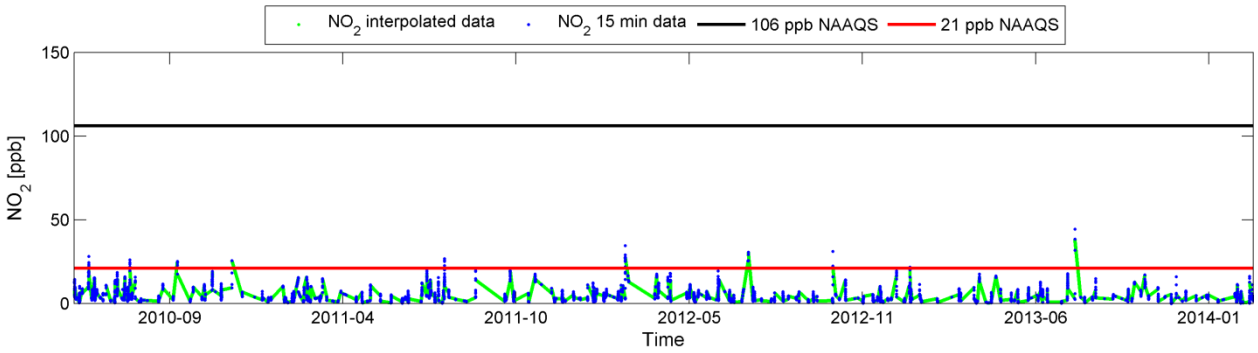

(c)

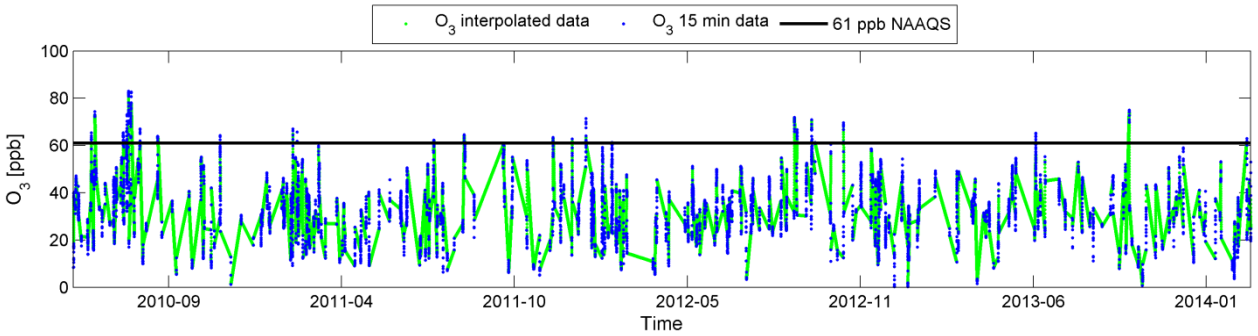

Figure 6 continues: The 15-min average *in situ* pollutant concentration data that was correlated with the arrival times of the selected back trajectories and linear interpolation of this data for (a) SO_2, (b) NO_2, (c) O_3, (d) CO and (e) PM_{10} for the entire sampling period. The NAAQS limits for the afore-mentioned atmospheric species are also indicated.

(d)

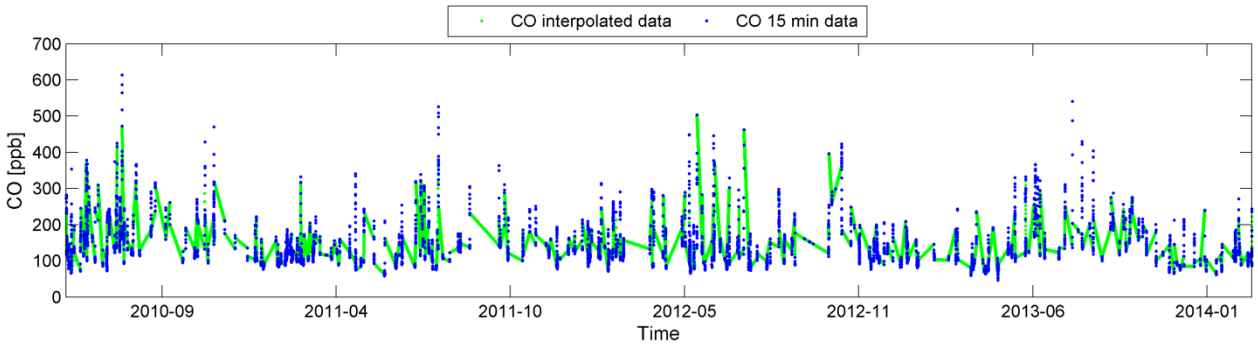

(e)

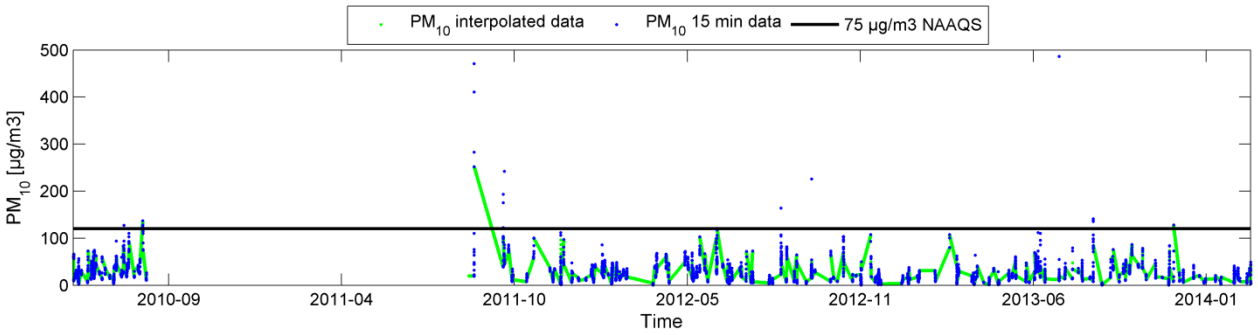

Figure 7: Comparison of mean pollutant concentrations in air masses that passed over the Vredefort Dome, with mean values reported for other continental sites in South Africa.

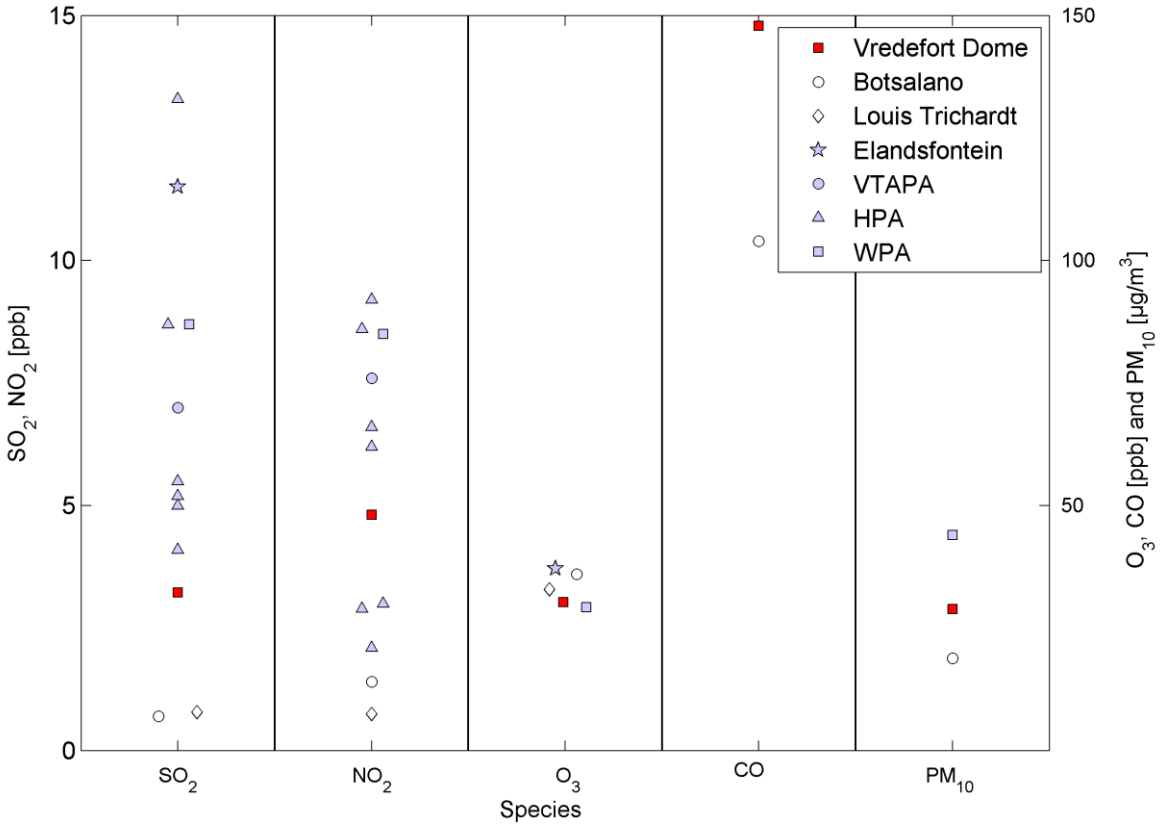

Figure 8: Differentiation of O_3 and PM_{10} normalised concentrations in air masses that complied with the selection criteria of passing over the Vredefort Dome, in terms of trajectories that had passed over the LPS region and those that had not passed over the LPS region.

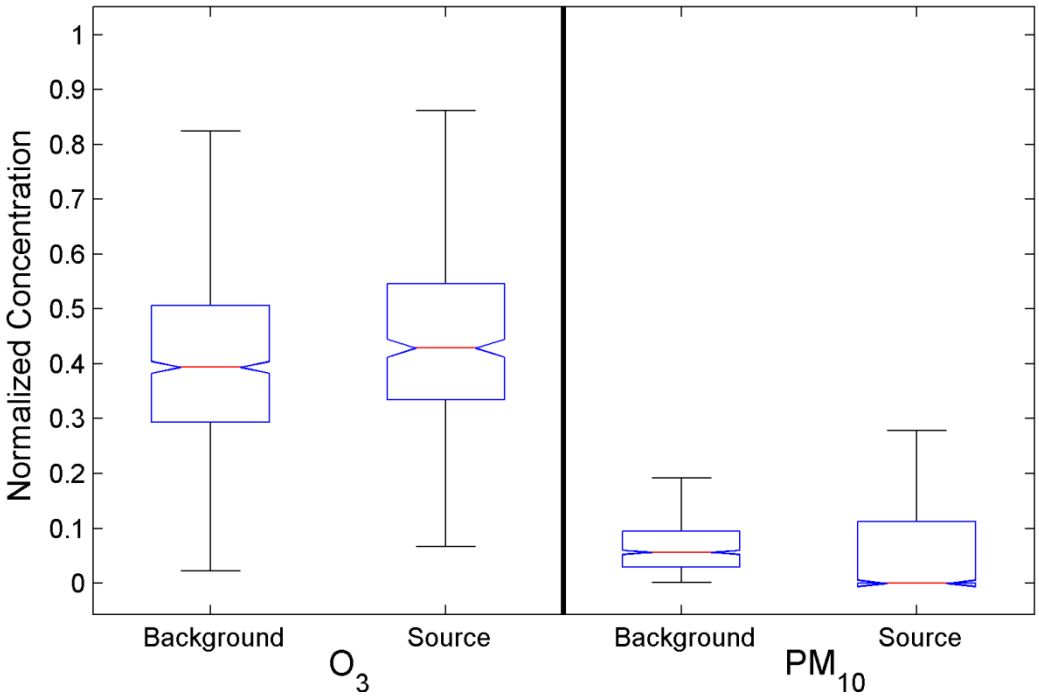

Figure 9: Monthly concentrations for (a) O_3, (b) CO (c) PM_{10} and (d) BC in air mass back trajectories that complied with the selection criteria during the sampling period.

(a)

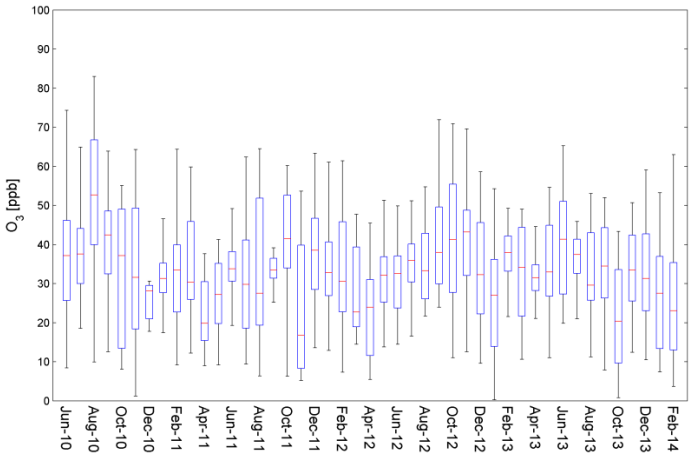

(b)

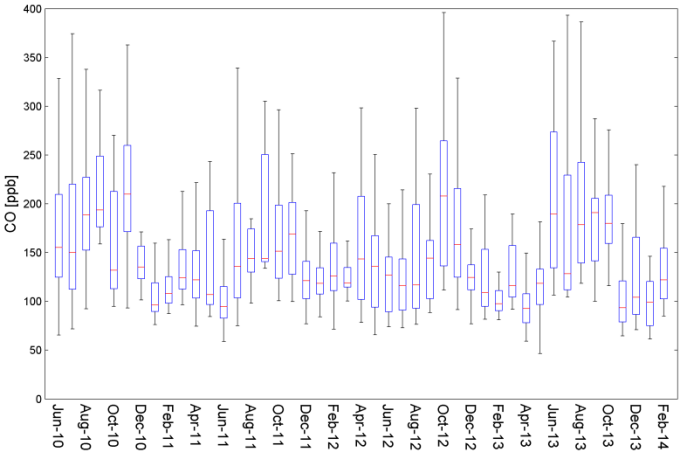

(c)

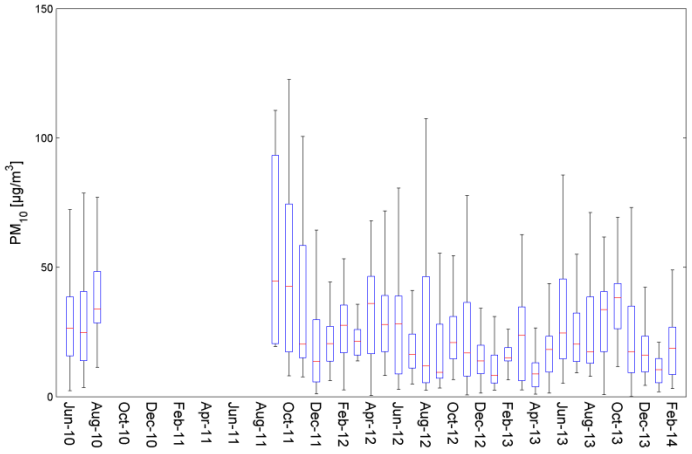

Figure 9 continues: Monthly concentrations for (a) O_3, (b) CO (c) PM_{10} and (d) BC in air mass back trajectories that complied with the selection criteria during the sampling period.

(d)

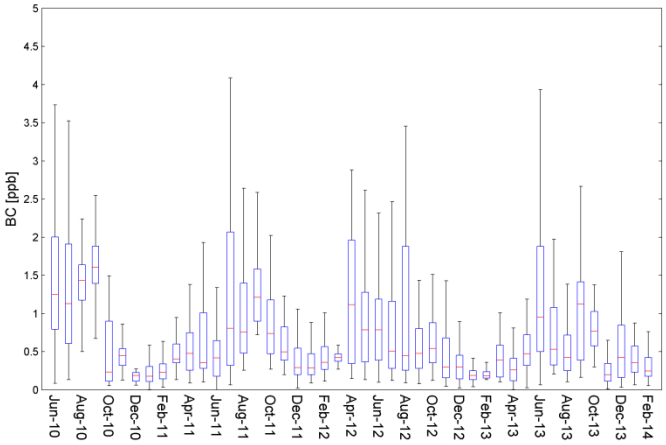

Table 1: Observed criteria pollutant concentrations compared with the current South African National Ambient Air Quality Standards (NAAQS)

South African National Ambient Air Quality Standards				Observed concentrations	
Pollutant	**Averaging period**	**Concentration, ppb (µg/m^3)**	**Frequency of exceedances per year**	**Frequency of exceedances per year**	**Mean concentration ppb (µg/m^3)**
SO_2	10 min	191 (500)	526	0	3.22 (8.43)
	1 hour	134 (350)	88	0	
	24 hours	48 (125)	4	0	
	1 year	19 (50)	0	0	
NO_2	1 hour	106 (200)	88	0	4.81 (9.05)
	1 year	21 (40)	0	0	
O_3	8 hour (moving average)	61 (120)	11	141	30.24 (59.37)
CO	1 hour	26 000 (30 000)	88	0	147.91 (170)
	8 hour (calculated from 1 hour averages)	8700 (10 000)		0	
PM_{10}	24 hours (2015)	(75)	4	17	(28.91)
	1 year (2015)	(40)		0	

Chapter 5

Conclusions and evaluation of study

5.1. Conclusions

This study is the first air quality assessment for the Vredefort Dome world heritage site. By identifying back trajectories that had passed over the Dome and thereafter not passing over significant source areas before arriving at the Welgegund atmospheric monitoring station, proxies for air quality could be determined over the Vredefort Dome. The following main deductions could be made from the results:

- The method had some limitations, since the frequencies of back trajectories that complied with the selection criteria were limited and those that did comply, mostly passed over the cleaner south-western sector from the Vredefort Dome. Additionally, dilution during transport and aging of air masses after passing over the Vredefort Dome before arriving at Welgegund could also affect the pollutant levels observed. Overlay back trajectory maps indicated that air quality in the Vredefort Dome is likely to be impacted significantly by the known priority areas and the Johannesburg-Pretoria (Jhb-Pta) megacity. Therefore, the air quality proxies presented in this study can be considered as an underestimation of pollutant levels.
- By comparing the results obtained during this study with the National Ambient Air Quality Standards (NAAQS), it is evident that O_3 and PM_{10} exceeded the NAAQS limits. O_3 is a regional problem, while PM_{10} mostly originates from industries, household combustion and savannah/grassland fires.

- Although there were no exceedances recorded for SO_2 and NO_2 in the air masses complying with the selection criteria, it is highly likely that such exceedances will occur over the Vredefort Dome, but that the afore-mentioned method limitation prevented observations thereof.

5.2. Project evaluation

Each objective is subsequently considered and the successes and/or shortcomings are discussed:

Objective i) Identifying back trajectories passing over the Vredefort Dome

The 96-hour back trajectories, arriving hourly, were generated with HYSPLIT 4.8 (HYbrid Single-Particle Lagrangian Intergrated Trajectory) for the entire measurement period with an arrival height of 100 m. Overlay back trajectory maps were generated by superimposing individual back trajectories generated in HYSPLIT with a fit-for-purpose MATLAB script on maps that were divided into 0.2 X 0.2°grid cells (Chapter 4, Figure 4). Additionally, individual back trajectories were sorted according to specific selection criteria that allowed the identification of trajectories that had passed over the Vredefort Dome area before arriving at Welgegund, but did not pass over significant sources after passing over the Dome (Paragraph 3.4 and Figure 3.2).

Objective ii) Linking in situ atmospheric measurements of pollutant species conducted at the Welgegund monitoring station with the identified back trajectories

The 15 min average data of the *in situ* pollutant species measured at Welgegund was linked to every selected hourly arriving back trajectory with the two 15 min average before the hourly arrival time, as well as the two 15 min averages after the hourly back trajectory arrival time.

Therefore, each selected back trajectory was associated with four 15 min averages of the *in situ* measurements.

Certain averaging periods (associating with the NAAQS (Paragraph 2.3, Table 2.1) were calculated form the measured data for each of the pollutant species, i.e. SO_2, NO_2, O_3, CO and PM_{10}. For the legislation relating to a 10 min averaging period, i.e. only for SO_2, each of the four 15 min average SO_2 values measured at Welgegund that were associated with the selected back trajectory arrival time could be compared to the legislative requirement. Similarly, for the one-hour legislatively averaging periods for SO_2, NO_2 and CO, the selected back trajectory arrival times were correlated directly with the average of the four 15 min values associated with the back trajectory arrival time. However, for the longer legislative averaging periods, e.g. eight and 24 hours, it was not that simple, since the frequency of back trajectories that complied with the first selection criteria was not very high. In order to at least make estimates of such possible exceedances, the 15 min average data that was correlated to the arrival times of the selected back trajectories was linearly interpolated and the averages for each specie was calculated from the interpolated data.

Objective iii) Comparing the measured pollutant concentrations that were linked with the appropriate back trajectory arrival times with National Ambient Air Quality Standards (NAAQS)

The comparison between the measured concentrations and the NAAQS showed that SO_2, NO_2 and CO did not exceed any limits. Although there were no exceedances for SO_2 and NO_2 it is likely that such exceedances will occur, but these were not detected due to the method limitations. In contrast, O_3 and PM_{10} exceeded the limit values. O_3 exceeded the eight-hour moving average standard of 61 ppb on average 141 times per year and PM_{10} exceeded the 24-hour average standard of 75µg/m^3 17 times per year.

Objective iv) Identifying possible trends in pollutant concentrations and relate these to possible sources

There were no distinctive seasonal patterns observed for SO_2 and NO_2. This can be attributed to the relatively low frequencies of air masses that were identified according to the selection criteria. Additionally, SO_2 and NO_2 in the South African interior mostly originate from continuous operating industrial sources. For O_3, CO, PM_{10} and BC, more distinct seasonal patterns were observed. The highest levels of O_3 concentrations occurred during the late spring and early summer months. The main contributing factors were identified to be higher levels of O_3 precursors from savannah and grassland fires, as well as the onset of longer daylight hours during this time of the year. O_3 was identified as a regional problem, not restricted to the Vredefort Dome area. CO and BC peaked mostly during the drier and colder months, which coincided with savannah and grassland fire frequencies, as well as household combustion for space heating. PM_{10} also peaked during similar periods than CO and BC, indicating similar sources.

Objective v) Presenting an assessment of the air quality over the Vredefort Dome based on the above-mentioned air quality proxies indicating what interventions are required in future

From the results presented in this study (Chapter 4, Paragraph 4), it is evident that the back trajectories that complied with the selection criteria mostly passed over the cleaner south-western sector from the Vredefort Dome. The overlay back trajectory map of trajectories arriving at the Vredefort Dome indicated that air quality in the Dome is likely to be impacted significantly by the known priority areas and the Jhb-Pta megacity. Therefore, the air quality proxies presented in this study can be considered as an underestimation of pollutant levels. Notwithstanding these limitations, the study indicated that there are air quality problems in the Vredefort Dome area. In order to quantify this better and to track possible future

improvements, a continuously operated air quality station needs to be established within the proclaimed area.

For the species that exceeded the NAAQS limits, i.e. O_3 and PM_{10}, certain interventions are required to address the problems in future. O_3 remains a regional problem in South Africa. In order to reduce O_3 concentrations, O_3 precursor (NO_2, VOCs and CO) concentrations must be reduced. This implies interventions for industrial activities, the vehicular fleet, as well as savannah and grassland fire emissions. In this study, it seemed that PM_{10} over the Dome was significantly influenced by household combustion, as well as savannah and grassland fire emissions. In order to address household combustion emissions, social and economic transformations in South Africa need to be accomplished, which are linked to the economic success and -growth of the country.

5.3. Future perspectives

- In order to obtain a better air quality assessment and track possible future improvements over the Vredefort Dome, it would be recommended to measure atmospheric species within the Vredefort Dome.
- Instead of using the linear interpolation method applied for the missing values due to the low frequency of back trajectories that complied with the selection criteria, a multi-linear regression analysis can be used to determine the missing values more accurately.

Bibliography

Air Resources Laboratory, National Oceanic and Atmospheric Administration (NOAA). 2015. http://www.arl.noaa.gov/ Date of access: 5 Mar. 2014.

API, Advanced Pollution Instrumentation. 1999. Model 200AU - Nitrogen Oxides Analyzer. San Diego.

ATKINSON, R. 2000. Atmospheric chemistry of VOCs and NOx. *Atmospheric Environment*, 34:2063-2101.

BERNSTEIN, J.A., ALEXIS, N., BARNES, C., BERNSTEIN, I.L., NEL, A., PEDEN, D., DIAZ-SANCHEZ, D., TARLO, S.M. & WILLIAMS, P.B. 2004. Health effects of air pollution. *Journal of Allergy and Clinical Immunology.*, 114:1116-1123.

BEUKES, J.P., VAKKARI, V., VAN ZYL, P.G., VENTER, A.D., JOSIPOVIC, M., JAARS, K., TIITTA, P., KULMALA, M., WORSNOP, D., PIENAAR, J.J., VIRKKULA, A. & LAAKSO, L. 2013. Source region plume characterisation of the interior of South Africa as observed at Welgegund. *Clean Air Journal*, 23:7-10.

BEUKES, J.P., VENTER, A.D., JOSIPOVIC, M., VAN ZYL, P.G., VAKKARI, V., JAARS, K., DUNN, M. & LAAKSO, L. 2015. Automated continuous air monitoring. (*In* FORBES, P., *ed*. Monitoring Of Air Pollutants – Sampling, Sample, Preparation And Analytical Techniques, Elsevier. In press.)

BOND, T.C., DOHERTY, S.J., FAHEY, D.W., FORSTER, P.M., BERNTSEN, T., DEANGELO, B.J., FLANNER, M.G., GHAN, S., et al. 2013. Bounding the role of black carbon in the climate system: A scientific assessment. *Journal of Geophysical Research*, 118:5380-5552.

BOND, T.C., STREETS, D.G., YARBER, K.F., NELSON, S.M., WOO, J.-H. & KLIMONT, Z. 2004. A technology-based global inventory of black and organic carbon emissions from combustion. *Journal of Geophysical Research*, 109:D14203.

BOOYENS, W., VAN ZYL, P.G., BEUKES, J.P., RUIZ-JIMENEZ, J., KOPPERI, M., RIEKKOLA, M., JOSIPOVIC, M., VENTER, A.D., JAARS, K., LAAKSO, L., VAKKARI, V., KULMALA, M. & PIENAAR, J.J. 2015. Size-resolved characterisation of organic compounds in atmospheric aerosols collected at Welgegund, South Africa. *Journal of Atmospheric Chemistry*, 72:46-64.

BRINK, M.C., WAANDERS, F.B., BISSCHOFF, A.A. & GAY, N.C. 2000. The Foch Thrust-Pochefstroom Fault structural system, Vredefort, South Afirca: a model for impact-related tectonic movement over a pre-existing barrier. *Journal of African Earth Sciences*, 30:99-117.

Business Dictionary. 2015. http://www.businessdictionary.com/definition/air-pollution.html Date of access: 1 Sep. 2015.

CONNELL, D.W. 2005. Basic Concepts of Environmental Chemistry. 2nd ed. Boca Raton: Tylor and Francis Group. 458p.

DALY, A. & ZANNETTI, P. 2007. An Introduction of Air Pollution - Definitions, Classifications, and History. (*In* ZANNETTI, P., AL-AJMI, D. & AL-RASHIED, S., *eds*. Ambient air Pollution, The Arab School for Science and Tegnology (ASST) and The EnviroComp Institue. 1-14 p.)

DEUTSCH, A., GRIEVE, R.A.R., AVERMANN, M., BISCHOFF, C., BROCKMEYER, P., BUHL, D., LAKOMY, R., MULLER-MOHR, V., OSTERMANN, M. & STOFFLER, D. 1995. The Sudbury Structure (Ontario, Canada); a tectonically deformed multi-ring impact basin. *Geologische Rundschau,* 84:697-709.

Earth Impact Database. 2011. http://www.passc.net/EarthImpactDatabase/Agesort.html Date of access: 21 Oct. 2015.

ENGELBRECHT, J.C. 2013. Vredefort Dome World Heritage Site – Air Quality Management Plan. http://www.docstoc.com/docs/69775804/Air-Quality-Management-plan Date of access: 22 Apr. 2014.

ENVIRONMENT, SA. 1999. O3 41M UV Photometry Ozone Analyzer. Poissy.

Environmental Protection Agency (EPA). 2009. Regulatory Actions. http://www3.epa.gov/airquality/sulfurdioxide/actions.html Date of access: 8 Aug. 2015.

Environmental Protection Agency (EPA). 2015. http://www3.epa.gov/airquality/nitrogenoxides/ Date of access: 7 Aug. 2015.

Environmental Protection Agency (EPA). 2015. http://www3.epa.gov/airquality/sulfurdioxide/ Date of access: 10 Aug. 2015.

ERNST, A. & ZIBRAK, J.D. 1998. Carbon monoxide poisoning. *The New England Journal of Medicine*, 339:1603-1608.

FABIAN, P. & PRUCHNIEWICZ, P.G. 1977. Meridional distribution of ozone in tropsphere and its seasonal-variations. *Journal of Geophysical Researh*, 82:2063.

FENGER, J. 2009. Urban air pollution. (*In* HEWITT, C.N. & JACKSON, A.V., *eds*. Atmospheric Science for Environmental Scientists. Chichester, W. Sussex: Wiley-Blackwell. 242-267 p.)

FISHMAN, J. 2003. Overview: Atmospheric Chemistry. (*In* POTTER, T.D. & COLMAN, B.R., *eds*. Handbook of Weather, Climate and Water. Hoboken, N.J.: John Wiley and Sons. 3-28 p.)

FLEMING, G. & VAN DER MERWE, M. 2004. Spacial Disaggregation of Greenhouse Gas Emission Inventory Data for Africa South of the Equator.

http://gis.esri.com/library/userconf/proc00/professional/papers/PAP896/p896.htm Date of access: 1 Sep. 2015.

FRENCH, B. M. 1998. Traces of Catastrophe: A Hanbook of Shock-Metamorphic Effects in Terrestrial Meteorite Impact Structures. Houston: Lunar and Planetary Institute. 120 p.

GIBSON, R.L. & REIMOLD, W.U. 1999. The significance of the Vredefort Dome for the thermal and structural evolution of the Witwatersrand Basin, South Africa. *Mineralogy and Petrology*, 66:5-23.

GIERENS, R., LAAKSO, L., MOGENSEN, D., VAKKARI, V., BEUKES, J.P., VAN ZYL, P.G., GUENTHER, A., PIENAAR, J.J. & BOY, M. 2014. Modelling new particle formation events on South African savannah. *South African Journal of Science.*, 110:1-12.

GRIEVE, R.A.F., SMITH, R.J. & THERRIAULT, A. 1995. The record of terrestrial impact cratering. *Geological Society of America*, 5:193-196.

HARRIS, C., FOURIE, D. S. & FAGERENG, A. 2013. Stable Isotope for impact-related Pseudotachylite formation at Vredefort by local melting of dry rocks. *South African Journal of Geology*, 116.1:101-118.

HIRSIKKO, A., VAKKARI, V., TIITTA, P., HATAKKA, J., KERMINEN, V.-M., SUNDSTRöM, A.-M., BEUKES, J.P., MANNINEN, H.E., KULMALA, M. & LAAKSO, L. 2013. Multiple daytime nucleation events in semi-clean savannah and industrial environments in South Africa: analysis based on observations. *Atmospheric Chemistry and Physics*, 13:5523-5532.

HIRSIKKO, A., VAKKARI, V., TIITTA, P., MANNINEN, H.E., GAGNE, S., LAAKSO, H., KULMALA, M., MIRME, A., MIRME, S., MABASO, D., BEUKES, J.P. & LAAKSO, L. 2012. Characterisation of sub-micron particle number concentrations and formation events in the western Bushveld Igneous Complex, South Africa. *Atmospheric Chemistry and Physics*, 12:3951-3967.

HYVäRINEN, A.-P., VAKKARI, V., LAAKSO, L., HOODA, R.K., SHARMA, V.P., PANWAR, T.S., BEUKES, J.P., VAN ZYL, P.G., JOSIPOVIC, M., GARLAND, R.M., ANDREAE, M.O., PÖSCHL, U. & PETZOLD, A. 2013. Correction for a measurement artefact of the Multi-Angle Absorption Photometer (MAAP) at high black carbon mass concentration levels. *Atmospheric Measurement Techniques*, 6:81-90.

Intergovernmental Panel on Climate Change (IPCC). 2007. Cliamte Change 2007: The Physical Science Basis. http://www.ipcc.ch/publications_and_data/ar4/wg1/en/contents.html Date of access: 26 Aug. 2015.

Intergovernmental Panel on Climate Change (IPCC). 2013. Climate Change 2013: The Physical Science Basis. http://www.ipcc.ch/report/ar5/wg1/ Date of access: 12 Aug. 2015.

Intergovernmental Panel on Climate Change (IPCC). 2014. Climate Change 2014: Synthesis report. http://www.ipcc.ch/report/ar5/syr/ Date of access: 30 Jul. 2015.

JAARS, K., BEUKES, J.P., VAN ZYL, P.G., VENTER, A.D., JOSIPOVIC, M., PIENAAR, J.J., VAKKARI, V., AALTONEN, H., LAAKSO, H., KULMALA, M., TIITTA, P., GUENTHER, A., HELLEN, H., LAAKSO, L. & HAKOLA, H. 2014. Ambient aromatic hydrocarbon measurements at Welgegund, South Africa. *Atmospheric Chemistry and Physics*, 14:7075-7089.

JACOB, D.J. 2000. Heterogeneous chemistry and tropospheric ozone. *Atmospheric Environment*, 34:2131-2159.

JACOBSON, M. Z. 2001. Strong radiative heating due the mixing state of black carbon in atmospheric aerosols. *Nature*, 409:695-697.

JAIN, A. 2009. Global warming and climate change science. (*In* HEWITT, C.N. & JACKSON, A.V., *eds*. Atmospheric Science for Environmental Scientists. Chichester, W. Sussex: Wiley-Blackwell. 268-292 p.)

JAYARATNE, E.R. & VERMA, T.S. 2001. The impact of biomass burning on the environmental aerosol concentration in Gaborone, Botswana. *Atmospheric Environment*, 35:1821-1828.

JOSIPOVIC, M., ANNEGARN, H.J., KNEEN, M.A., PIENAAR, J.J. & PIKETH, S.J. 2010. Concentrations, distributions and critical level exceedance assessment of SO_2, NO_2 and O_3 in South Africa. *Environmental Monitoring and Assessment*, 171:181:196.

KAMPA, M. & CASTANAS, E. 2008. Human heatlh effects of air pollution. *Environmental Pollution*, 151:362-367.

KOCH, D. & DEL GENIO, A.D. 2010. Black Carbon semi-direct effects on cloud cover: review and synthesis. *Atmospheric Chemistry and Physics*, 10:7685-7696.

KUIK, F., LAUER, A., BEUKES, J.P., VAN ZYL, P.G., JOSIPOVIC, M., VAKKARI, V., LAAKSO, L. & FEIG, G.T. 2015. The anthropogenic contribution to atmospheric black carbon concentrations in southern Africa: a WRF-chem modeling study. *Atmospheric Chemistry and Physics*, 15:7309-7363.

LAAKSO, L., LAAKSO, H., AALTO, P.P., KERONEN, P., PETÄJÄ, T., NIEMINIEN, T., POHJA, T., SIIVOLA, E., KULMALA, M., KGABI, N., MOLEFE, M., MABASO, D., PHALATSE, D., PIENAAR, K. & KERMINEN, V.-M. 2008. Basic characteristics of atmospheric particles, trace gases and meteorology in relatively clean Southern Africa Savannah environment. *Atmopheric Chemistry and Physics*, 8:4823-4839.

LAAKSO, L., VAKKARI, V., VIRKKULA, A., LAAKSO, H., BACKMAN, J., KULMALA, M., BEUKES, J.P., VAN ZYL, P,G., TITTA, P., JOSIPOVIC, M., PIENAAR, J.J., CHILOANE, K., GILARDONI, S., VIGNATI, E., WIEDENSOHLER, A., TUCH, T., BIRMILI, W., PIKETH, S., et al. 2012. South African EUCAARI measurements: seasonal variation of trace gases and aerosol optical properties. *Atmospheric Chemistry and Physics*, 12:1847-1864.

LAZARIDIS, M. 2008. Organic Aerosols. (*In* COLBECK, I., *ed*. Environmental Chemistry of Aerosols. Oxford, UK: Blackwell. 91-115 p.)

LOURENS, A.S.M. 2008. Spatial and Temporal assessment of pollutants in the Highveld Priority Area, South Africa. Potchefstroom: NWU. (Dissertation – M.Sc.) 99p.

LOURENS, A.S., BEUKES, J.P., VAN ZYL, P.G., FOURIE, G.D., BURGER, J.W., PIENAAR, J.J., READ, C.E. & JORDAAN, J.H. 2011. Spacial and temporal assessment of gaseous pollutants in the Highveld of South Africa. *South African Journal of Science*, 107:1-8.

LOURENS, A.S.M., BUTLER, T.M., BEUKES, J.P., VAN ZYL, P.G., BEIRLE, S., WAGNER, T.K., HEUE, K., PIENAAR, J.J., FOURIE, G.D. & LAWRENCE, M.G. 2012. Re-evaluating the NO_2 hotspot over the South African Highveld. *South African Journal of Science*, 108:1-6.

MAENHAUT, W., SALMA, I., CAFMEYER, J., ANNEGARN, H.J. & ANDREAE, M.O. 1996. Regional atmospheric aerosol composition and sources in the eastern Transvaal, South Africa, and impact of biomass burning. *Journal of Geophysical Research*, 101:631-650.

MCCONNEL, J.R., EDWARDS, R., KOK, G.L., FLANNER, M.G., ZENDER, C.S., SALTZMAN, E.S., BANTA, J.R., PASTERIS, D.R., CARTER, M.M. & KAHL, J.D.W. 2007. 20th-Century Industrial Black Carbon Emissions Altered Arctic Climate Forcing. *Science*, 317:1381-1384.

MINTER, W.E.L., GOEDHART, M., KNIGHT, J. & FRIMMEL, H.E. 1993. Morphology of Witwatersrand gold grains from the Basal Reef: evidence for their detrital origin. *Economic Geology*, 88:273-248.

MONKS, P. & LEIGH, R. 2009. Tropospheric chemistry and air pollution. (*In* HEWITT, C.N. & JACKSON, A.V., *eds*. Atmospheric Science for Environmental Scientists. Chichester, W. Sussex: Wiley-Blackwell. 114-145 p.)

NOVELLI, P. 2003. Carbon monoxide in the atmosphere. (*In* POTTER, T.D. & COLMAN, B.R., *eds*. Handbook of weather, climate and water. Hoboken, N.J.: John Wiley and Sons, Inc. 78-88 p.)

ONLINE OXFORD ENGLISH DICTIONARY. 2015. World Heritage Site. http://www.oxforddictionaries.com/definition/english/World-Heritage-Site Date access: 10 Mar. 2014.

PENNER, J.E., ANDREAE, M. Annegarn, H., BARRIE, L., FEICHTER, D., HEGG, D., JAYARAMAN, A., LEAITCH, R., MURPHY, D., NGANGA, J. & PITARI, G. 2001. Aerosols, their Direct and Indirect Effects. (*In* HOUGHTON, J.T., DING, Y., GRIGGS, D.J., NOGUER, M., VAN DER LINDEN, P.J., DAI, X., et al, *eds*. Climate Change 2001: The Scientific Basis. Contribution of Working Group I to the Third Assessment Report of the

Intergovernmental Panel on Climate Change, Cambridge, UK, & NY, USA: Cambridge University Press. 298-348 p.)

PIENAAR, J.J. & HELAS, G. 1996. The kinetics of chemical processes affecting acidity in the atmosphere. *South African Journal of Sciences*, 128-131.

PÖSCHL, U. 2005. Atmospheric Aerosols: Composition, Transformation, Climate and Health Effects. *Angewandte Chemie International Edition*, 44:7520-7540.

REIMOLD, W.U. 2011. The Vredefort Dome: Centre of the Wold's Largest Meteorite Impact Structure. http://www.parys.co.za/parys/vredefort-dome.html Date access: 18 Mar. 2015.

REIMOLD, W.U. & GIBSON, R.L. 1996. Geology and evolution of the Vredefort Impact Structure, South Africa. *Journal of African Earth Sciences*, 23:125-162.

ROBINSON, E. & ROBBINS, R.C. 1970. Gaseous Nitrogen Compound Pollutants from Urban and Natural Sources. *Journal of the Air Pollution Control Association*, 20:303-306.

ROSEN, H., HANSEN, A.D.A., GUNDEL, L. & NOVAKOV, T. 1978. Identification of the optically absorbing component in urban aerosols. *Applied Optics*, 17:3859-3861.

ROSS, K.E., PIKETH, S.J., BRUINTJES, T., BURGER, R.P., SWAP, R.J. & ANNEGARN, H.J. 2003. Spatial and seasonal variations in CCN distribution and the aerosol-CCN relationship over southern Africa. *Journal of Geophysical Research*, 108:17-1 - 17-18.

SOUTH AFRICA. 2006. Declaration of the Vaal Triangle Air-shed Priority Area in terms of Section 18(1) of the National Environmental Management: Air Quality Act 2004, (ACT NO. 39 OF 2004). *Government gazette*, 28732: 21 Apr. Available: Department Environmental Affairs RSA. Date of acces: 15 Oct. 2015.

SOUTH AFRICA. 2007. Declaration for the Highveld as Priority Area in terms of Section18(1) of the National Environmental Management: Air Quality Act, 2004 (ACT NO. 39 OF 2004). *Government gazette*, 35018: 23 Nov. Available: Department Environmental Affairs RSA. Date of access: 15 Oct. 2015.

SOUTH AFRICA. 2007. World Heritage Convention Act, 1999 (NO. 49 OF 1999) Proclamation of Vredefort Dome as World Heritage Site. *Government gazette*, 30590: 18 Dec. Available: South African Government. Date of access: 21 Mar. 2014.

SOUTH AFRICA. 2009. National Environment Management: Air Quality Act, 2004 (ACT NO. 39 OF 2004). *Government gazette*, 32816: 24 Dec. Available: Department Environmental Affairs RSA. Date of access: 15 Oct. 2015.

SOUTH AFRICA. 2009. National Environmental Management: Air Quality Act, 2004 (ACT NO. 39 OF 2004) Regulations for implementing and enforcing the Vaal Triangle AirShed Priority Area Air Quality Management Plan. *Government gazette*, 32254: 29 May.

Available: Department Environmental Affairs RSA – Gazette Notices. Date of access: 15 Oct. 2015.

SOUTH AFRICA. 2011. National Environmental Management: Air Quality Act, 2004 (ACT NO. 39 OF 2004) Highveld Priority Area Air Quality Management Plan. *Government gazette*, 35072: 2 Mar. Available: Department Environmental Affairs RSA – Gazette Notices. Date of access: 15 Oct. 2015.

SOUTH AFRICA. 2012. National Environmental Management: Air Quality Act, 2004 (ACT NO. 39 OF 2004) Declaration of the Waterberg National Priority Area. *Government gazette*, 35435: 15 Jun. Date of access: 15 Oct. 2015.

SAHU, L.K., KONDO, Y., MIYAZAKI, Y. Pongkiatkul, P. & KIM OANH, N.T. 2011. Seasonal and diurnal variations of black carbon and organic carbon aerosols in Bangkok. *Journal of Geophysical Research*, 116:D15302.

SEINFIELD, J.H. & PANDIS, S.P. 2006. Atmospheric Chemistry and Physics: From Air Pollution to Climate Chane. 2nd ed. N. J: John Wiley and Sons, Inc. 1225p.

SHALLCROSS, D. 2009. Biogeochemical cycles. (*In* HEWITT, C.N. & JACKSON, A.V., *eds*. Atmospheric Science for Environmental Scientists. Chichester, W. Sussex: Wiley-Blackwell. 83-113 p.)

SMITH, M.S. 1982. Dissimilatory Reduction of NO_2^- to NH_4^+ and N_2O by a Soil Citrobacter sp. *Applied and Environmental Microbiology*, 43:854-860.

SMITH, S.J., VAN AARDENNE, J., KLIMONT, Z., ANDRES, R.J., VOLKE, A. & DELGADO ARIAS, S. 2011. Anthropogenic sulfur dioxide emissions: 1850-2005. *Atmospheric Chemistry and Physics*, 11:1101-1116.

SOUTH COAST AIR QUALITY MANAGEMENT DISTRICT, Monitoring and Analysis Division. 2012. Horiba Ambient CO Monitor APMA-360, Standard Operating Procedure.

SPRAY, J. 2015. Earth Impact Database. http://www.passc.net/EarthImpactDatabase/ Date of access: 22 Sep. 2015.

SWAP, R.J., ANNEGARN, H.J., SUTTLES, J.T., KING, M.D. & PLATNICK, S. 2003. Africa burning: A thematic analysis of the Southern African Regional Science Initiative (SAFARI 2000). *Journal of Geophysical Research*, 108:8465.

THERMO ENVIRONMENTAL INSTRUMENTS. 1989. Model 43S SO2 Analyzer.

THERMO FISHER SCIENTIFIC. 2007. Model 5012 MAAP - Multi Angle Absorption Photometer. Franklin.

THERMO FISHER SCIENTIFIC. 2007. Model 5030 SHARP - Synchronized Hybrid Ambient Real-time Particulate Monitor. Franklin.

THOMPSON, A.M., BALASHOV, N.V., WITTE, J.C., COETZEE, J.G.R., THOURET, V. & POSNY, F. 2014. Tropospheric ozone increases over the southern Africa region: bellwether for rapid growth in Southern Hemisphere pollution?. *Atmospheric Chemistry and Physics*, 14:9855-9869.

TIITTA, P., VAKKARI, V., JOSIPOVIC, M., CROTEAU, P., BEUKES, J.P., VAN ZYL, P.G., VENTER, A.D., JAARS, K., PIENAAR, J.J., NG, N.L., CANAGARATNA, M.R., JAYNE, J.T., KERMINEN, V.-M., KULMALA, M., LAAKSONEN, A., WORSNOP, D.R. & LAAKSO, L. 2014. Chemical composition, main sources and temporal variability of PM_1 aerosols in southern African grassland. *Atmospheric Chemistry and Physics Discussions*, 13:15517-15566.

United Nations, Educational, Scientific and Cultural Organization (UNESCO). 2015. World Heritage List. http://whc.unesco.org/en/list/ Date of access: 6 Oct. 2015.

United Nations, Educational, Scientific and Cultural Organization (UNESCO). 2015. World Heritage Scanned Nomination. http://whc.unesco.org/en/list/1162/documents/ Date of access: 6 Oct. 2015.

VAKKARI, V., BEUKES, J.P., LAAKSO, H., MABASO, D., PIENAAR, J.J., KULMALA, M. & LAAKSO, L. 2013. Long-term observations of aerosol size distributions in semi-clean and polluted savannah in South Africa. *Atmospheric Chemistry and Physics*, 13:1751-1770.

VAKKARI, V., KERMINEN, V.-M., BEUKES, J.P., TIITTA, P., VAN ZYL, P.G., JOSIPOVIC, M., VENTER, A.D., JAARS, K., WORSNOP, D.R., KULMALA, M. & LAAKSO, L. 2014. Rapid Changes in Biomass Burning Aerosols by Atmospheric Oxidation. *Geophysical Research Letters*, 41:2644-2651.

VAKKARI, V., LAAKSO, H., KULMALA, M., LAAKSONEN, A., MABASO, D., MOLEFE, N. & LAAKSO, L. 2011. New particle formation events in semi-clean South African savannah. *Atmospheric Chemistry Physics*, 11:3333-3346.

VAN ZYL, P.G., BEUKES, J.P., DU TOIT, G., MABASO, D., HENDRIKS, J., VAKKARI, V., TIITTA, P., PIENAAR, J.J., KULMALA, M. & LAAKSO, L. 2014. Assessment of atmospheric trace metals in the western Bushveld Igneous Complex, South Africa. South African Journal of Science, 110:1-11.

VENTER, A.D. 2011. Air quality assessment of the industrialized western Bushveld Igneous Complex. Potchefstroom: NWU. (Dissertation – M.Sc.) 85p.

VENTER, A.D., VAKKARI, V., BEUKES, J.P., VAN ZYL, P.G., LAAKSO, H., MABASO, D., TIITTA, P., JOSIPOVIC, M., KULMALA, M., PIENAAR, J.J. & LAAKSO, L. 2012. An air quality assessment in the industrialised western Bushveld Igneous Complex, South Africa. *South Africa Journal of Science*, 108:1-10.

WESTCOTT, G., TACKE, M., SCHOEMAN, N. & MORGAN, N. 2007. Impala Platinum Smelter, Rustenburg - an integrated smelter off-gass treatment solution. *The Journal of the Southern African Institute of Mining and Metallurgy*, 107:281-287.

WILLIAMS, P.I. & BALTENSPERGER, U. 2009. Particulate matter in the atmosphere. (*In* HEWITT, C.N. & JACKSON, A.V., *eds*. Atmospheric Science for Environmental Scientists. Chichester, W. Sussex: Wiley-Blackwell. 168-197 p.)